Germline-Encoded Affinity for Cognate Antigen Enables Vaccine Amplification of a Human Broadly Neutralizing Response against Influenza Virus

HHS Public Access

Author manuscript

Immunity. Author manuscript; available in PMC 2020 October 15.

Published in final edited form as:

Immunity. 2019 October 15; 51(4): 735–749.e8. doi:10.1016/j.immuni.2019.09.001.

Germline-encoded affinity for cognate antigen enables vaccine-amplification of a human broadly neutralizing response against influenza virus

Maya Sangesland[1], **Larance Ronsard**[1], **Samuel W. Kazer**[1,2,3], **Julia Bals**[1], **Seyhan Boyoglu-Barnum**[4], **Ashraf S. Yousif**[1], **Ralston Barnes**[5], **Jared Feldman**[1], **Maricel Quirindongo-Crespo**[5], **Patrick. M. McTamney**[6], **Daniel Rohrer**[5], **Nils Lonberg**[5], **Bryce Chackerian**[7], **Barney S. Graham**[4], **Masaru Kanekiyo**, **Alex K. Shalek**[1,2,3], **Daniel Lingwood**[1,8,*]

[1]The Ragon Institute of Massachusetts General Hospital, The Massachusetts Institute of Technology and Harvard University, 400 Technology Square, Cambridge, MA 02139

[2]Institute for Medical Engineering and Science (IMES), Department of Chemistry, and Koch Institute for Integrative Cancer Research, Massachusetts Institute of Technology, 77 Massachusetts Avenue, Cambridge, MA 02139

[3]Broad Institute of Massachusetts Institute of Technology and Harvard, 415 Main St, Cambridge, MA, 02142

[4]Vaccine Research Center, National Institute of Allergy and Infectious Diseases, National Institutes of Health, 40 Convent Drive, Bethesda, MD 20o92-3005

[5]Bristol-Myers Squibb, 700 Bay Rd, Redwood City, California, 94063-2478

[6]Medimmune, LLC, One MedImmune Way, Gaithersburg, MD 20878

[7]Department of Molecular Genetics and Microbiology, University of New Mexico School of Medicine, 2425 Camino de Salud, Albuquerque, NM 87106

[8]Lead Contact

Abstract

Antibody paratopes are formed by hypervariable complementarity-determining regions (CDRH3s) and variable gene-encoded CDRs. The latter shows biased usage in human broadly neutralizing antibodies (bnAbs) against both HIV and influenza virus, suggesting the existence of gene-

*Correspondence: dlingwood@mgh.harvard.edu.

Author Contributions

M.S. and D.L. designed the research studies; M.S., L.R., S.K., A.S.Y., J.B., S.B-B., J.F., R.B., M.Q-C., B.C., and D.L. performed the research; M.S., S.K., L.R., A.S.Y., S.B-B, R.B., D.R., P.M.M., N.L., B.C., B.S.G., M.K., A.S., and D.L analyzed data and M.S. and D.L. wrote the paper.

Competing Interests

Authors declare no competing interests. B.S.G. and M.K. are named as inventors of a pending patent application on stabilized influenza hemagglutinin stem region trimers and uses thereof filed by National Institutes of Health.

endowed targeting solutions that may be amenable to pathway amplification. To test this, we generated transgenic mice with human CDRH3 diversity but simultaneously constrained to individual user-defined human immunoglobulin variable heavy chain (V_H) genes, including IGHV1-69, which shows biased usage in human bnAbs targeting the hemagglutinin stalk of Group 1 influenza A viruses. Sequential immunization with a stalk-only hemagglutinin nanoparticle elicited Group 1 bnAbs, but only in IGHV1-69 mice. This V_H-endowed response required minimal affinity maturation, was elicited alongside pre-existing influenza immunity, and when IGHV1-69 B cells were diluted to match the frequency measured in humans. These results indicate that the human repertoire could in principle support germline-encoded bnAb elicitation using a single recombinant hemagglutinin immunogen.

Graphical Abstract

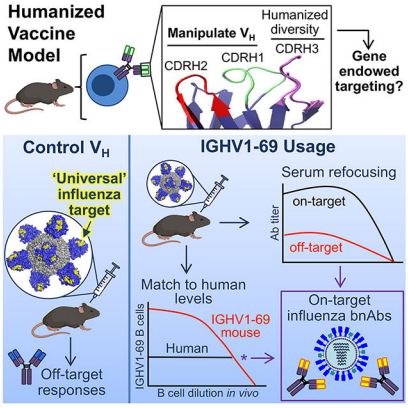

eTOC Blurb

Human broadly neutralizing antibodies (bnAbs) against influenza virus can be biased for VH-gene usage, suggesting gene-encoded development pathways. Sangesland et al. show that human IGHV1-69 B cell receptors impart natural affinity for a ‘universal’ vaccine target, enabling rapid bnAb responses in mice that were elicited using a rationally designed influenza immunogen.

Introduction

Antigen recognition relies on establishing biochemical affinity for a target epitope. For antibodies, the antigen-binding site is initially displayed by the germline B cell receptor (BCR) and is primarily formed by the hypervariable CDRH3, a centrally positioned antigen-binding loop unique to each B cell clone (Schroeder and Cavacini, 2010; Xu and Davis, 2000). While CDRH3 diversity facilitates broad recognition of diverse antigen structures, it often fails to explore the antigenic space equally, leading to dominant and subdominant antibody responses to different sites on the same antigen (Altman et al., 2015; Angeletti et al., 2017). Subdominant or low titer antibody responses can arise when the repertoire is endowed with low-frequency sources of on-target affinity, which are then unable to compete for selection in B cell germinal centers (Abbott et al., 2018; Dosenovic et al., 2018). While the physiochemical basis for low frequency targeting is unclear, it is a hallmark of human broadly neutralizing antibody (bnAb) responses against pathogens that ‘resist’ conventional

approaches to vaccination, including HIV and influenza virus (Altman et al., 2015; Peterhoff and Wagner, 2017). Here the capacity to expand CDRH3 solutions engaging the bnAb epitopes is difficult as they emerge in the repertoire both stochastically and with low reproducibility.

However, the germline antigen binding site is also formed by peripheral antibody V gene-encoded CDRs that can show biased usage in human bnAbs against both HIV and influenza virus. This suggests the existence of gene-endowed targeting solutions that could support pathway-based amplification through genetic reproducibility (Lerner, 2011; Peterhoff and Wagner, 2017; Zhou et al., 2015). To exploit this, germline B cell stimulating immunogens have been engineered which prime and expand the corresponding V_H-constrained HIV bnAb cell lineages within human V_H gene-knockin mice (Briney et al., 2016; Duan et al., 2018; McGuire et al., 2016; Tian et al., 2016; Verkoczy et al., and in mice containing adoptively transferred bnAb precursors (Abbott et al., 2018; Dosenovic et al., 2018; Dosenovic et al., 2019). However, these maturation pathways typically require exceptional levels of somatic hypermutation (SHM) to achieve broad neutralization of HIV, and the number and configuration of ‘shepherding’ immunogens needed to boost and mature the vaccine response to generate this activity remains unclear (Bonsignori et al., 2018; Peterhoff and Wagner, 2017; Umotoy et al., 2019). In this study, we demonstrate that a gene-encoded human CDR imparts natural cognate affinity for a conserved site of vulnerability on influenza virus, enabling rapid vaccine-amplification of a human V_H-constrained bnAb response, elicited by a single recombinant influenza immunogen.

Influenza virus remains a global health burden, producing a diversity of genetically distinct strains that are often poorly matched to seasonal vaccines (Erbelding et al., 2018; Paules and Subbarao, 2017; Petrie and Gordon, 2018). Influenza A viruses (IAV) account for the majority of hospitalizations and are a significant source of pandemic threats (Paules and Subbarao, 2017; Petrie and Gordon, . The major envelope glycoprotein hemagglutinin (HA) further sub-divides IAV into Group 1 and Group 2 viruses, and the discovery and ever-growing list of human bnAbs targeting conserved epitopes within the HA stalk region to attenuate infection across Group 1 and/or Group 2 viruses has stimulated great effort to enhance their elicitation by vaccination (Krammer et al., 2018; Nabel and Fauci, 2010; Wu and Wilson, 2017). While these antibodies have been operationally defined by their capacity to inhibit viral fusion with the host cell membrane *in vitro* (Cho and Wrammert, 2016; Wu and Wilson, 2017), their protective activity also appears to be mediated by antibody Fc functionalities (DiLillo et al., 2016; DiLillo et al., 2014; Kosik et al., 2019) that are enhanced when the stalk bnAb sites are targeted (He et al., 2016). However, the immune system has a distinctive preference for nonstalk HA epitopes, both following influenza infection or conventional vaccination with HA immunogens (Altman et al., 2015; Nabel and Fauci, 2010; Tan et al., 2019). Promising strategies to overcome this include sequential immunization with chimeric HA molecules to promote antibody boosting on conserved features (Krammer et al., 2018) and structure-based design of stalk-only displaying immunogens (Impagliazzo et al., 2015; Lu et al., 2014; Mallajosyula et al., 2014; Yassine et al., 2015). While these approaches have successfully elicited anti-stalk responses, vaccine-expansion of broadly neutralizing serum antibodies targeting the stalk bnAb epitopes has not been achieved.

Using *in vitro* reconstituted B cell-antigen interactions, we previously identified an unconventional V_H gene-centric mode of targeting by the germline BCR, wherein the hydrophobic CDRH2 loop encoded by the human V_H gene IGHV1-69 provides natural affinity to the Group 1 bnAb-epitope on the HA stalk, prior to antibody affinity maturation (Lingwood et al., 2012; Villar et al., 2016; Weaver et al., 2016). This reconstituted germline BCR specificity correlates with a subdominant but public human bnAb response that is biased for IGHV1-69 usage (>80%) and is panneutralizing across Group 1 IAVs (Avnir et al., 2014; Lerner, 2011; Pappas et al., 2014; Sui et al., 2009; Wheatley et al., 2015; Whittle et al., 2014). We hypothesized that V_H-endowed germline affinity for the influenza Group 1 bnAb epitope supplies the antibody repertoire with a natural, deterministic source of biochemical specificity for this target, and as such, a reproducible basis for focusing antibody responses upon it.

To test this hypothesis *in vivo*, we applied a humanized mouse recombineering platform (Fishwild et al., 1996; Lonberg et al., 1994; Xu and Davis, 2000) to generate transgenic mice in which antibody development was fully constrained to either IGHV1-69*01 or a control human V_H gene (IGHV1-2*02), but proceeded with humanized CDRH3 diversity. By systematically varying the V_H gene but maintaining CDRH3 diversity, we could experimentally define V_H contribution to human antibody epitope targeting as a function of immune challenge, as recorded by the serum antibody response where polyclonal targeting effects are critical for vaccine efficacy. Through this approach, we demonstrate that IGHV1-69 usage provides natural immunoreceptor activity for the Group 1 bnAb epitope, and identified rationally designed HA immunogen configurations that optimized serum antibody refocusing to this target and bnAb output through this property. This was assessed in both naive animals and when pre-existing immunity to influenza virus was present. Moreover, we measured the frequency of GHV1-69 bnAb precursors within human peripheral blood mononuclear cells (PBMCs) and performed B cell dilutions within our transgenic animals to cover this range. Collectively, our results indicate that the human repertoire could support gene-endowed bnAb elicitation using a single recombinant HA immunogen.

Results

CDRH2-centric contribution to the germline IGHV1-69 bnAb paratope.

CDRH2-directed recognition of the HA Group 1 bnAb epitope by the germline IGHV1-69 BCR defines a molecular basis for biased V_H gene usage in human bnAbs that target this site (Lingwood et al., 2012; Weaver et al., 2016). Selection of CDRH3 bearing tyrosine residues at Kabat positions 98100 is often seen in human IGHV1-69 bnAb lineages, as these residues provide a key polar contact to the target epitope (Avnir et al., 2014; Lerner, 2011; Pappas et al., 2014; Wheatley et al., 2015; Whittle et al., 2014). To define the importance of CDRH2 vs CDRH3 moieties in forming the germline paratope, we introduced mutations in these loops and assessed HA binding to three germline-reverted BCRs of human IGHV1-69 bnAbs. Mutation of the apex residue F54A in CDRH2 disrupted bnAb-epitope recognition by all germline BCRs, but removal of the polar tyrosine contact in CDRH3 by phenylalanine substitution was tolerated in two of the three antigen receptors (Figure S1A and S1B),

indicating a primary role for CDRH2 in forming the 'primordial' germline contact and suggesting that IGHV1-69 usage may be deterministic for bnAb epitope-targeting following immune challenge.

A transgenic model to experimentally test V_H-endowed epitope targeting as a function of immune challenge in vivo.

To experimentally test whether V_H affinity to the group 1 influenza bnAb epitope genetically endows for antibody responses against this site, we deployed humanized mice homozygous for the integrated HC2 locus, which provides for expression of near-normal and unrestricted human CDRH3 diversity and 100% restriction to specific V_H genes of interest (Fishwild et al., 1996; Lonberg et al., 1994; Xu and Davis, 2000). In this study, antibody responses were fully constrained to IGHV1-69*01 or IGHV1-2*02 (Figure 1A). Deep sequencing of the antigen naive IgM B cell repertoires in these animals revealed a CDRH3 chain length distribution and amino acid composition that mirrored the human repertoire (Figures 1B, 1C, S2A, and S2B), and was therefore unlike that of mice (DeWitt et al., 2016; Tian et al., 2016). Complete V_H gene restriction was also confirmed by sequencing BCRs from fluorescence-activated cell sorting (FACS)-isolated antigen naive B cells as well as >500 antigen-specific individual BCRs sequenced over the course of the study (Figure S2C). T cell and B cell numbers and frequencies were also comparable to wildtype (WT) C57BL/6 mice (Figures S2D and S2E). The Y98-100 containing CDRH3 sequences were also present in all of the genotypes at similar frequencies and were comparable to humans, indicating a lack of CDRH3 repertoire bias that would favor recognition of the group 1 bnAb epitope in any one genotype (Figure S2F). These models therefore allowed us to (1) experimentally vary V_H gene usage to causally define their individual contribution to epitope targeting by the serum antibody response, in which polyclonal target specificity is critical for vaccine efficacy; (2) assess this parameter in the human CDRH3 context, where this hypervariable loop is normally the primary determinant of antibody target specificity; and (3) rank order different immunogenic configurations of influenza HA for their capacity to elicit group 1 bnAbs within this framework (Figure 1D).

V_H-endowed targeting to the Group 1 bnAb epitope upon exposure to influenza virus.

We first assessed the capacity of our transgenic mice to elicit HA stalk bnAb-epitope targeting responses following infection with influenza virus. Accordingly, we infected our animals (C57Bl/6, IGHV1-69 and IGHV1-2 genotypes) with the H1N1 virus A/New Caledonia/20/1999 (NC99) (Figure 2A). This virus infects and propagates within mice but does not cause disease (Glaser et al., 2007). At two weeks post-infection (post-infection 1), we observed a robust primary IGHV1-69 IgG response targeting the Group 1 bnAb-epitope, as measured by serum antibody binding to a strain-matched HA trimer probe but not the HAΔstem, containing the I45R + T49R substitutions within HA2 that sterically occludes access to this site (Lingwood et al., 2012; Weaver et al., 2016) (Figure 2B and 2C). HA-specific IgG elicited in WT C57Bl/6 mice and IGHV1-2 animals were comparable in titer, but failed to engage the bnAb target (Figure 2C). IGHV1-69 therefore naturally endows a capacity to target the otherwise subdominant Group 1 bnAb epitope, as displayed by the native virion. However, we noted that secondary exposure to virus preferentially boosted off-target responses, as evidenced by elevated HA titers and loss of the differential in IGHV1-69

IgG reactivity to the HA vs HAΔstem probes at post-infection 2 and 3 time points (Figure 2C). This property could be recapitulated by sequentially immunizing with a recombinant HA displaying nanoparticle, in which eight copies of full length NC99 HA trimer were arrayed and stabilized by a self-assembling ferritin nanoparticle scaffold (HA-np) (Kanekiyo et al., 2013) (Figures 1D, 2A, and 2D). As with the viral display of HA, HA-np elicited antibodies with IGHV1-69-dependent targeting to the Group 1 bnAb epitope in the primary response, which were then outcompeted by off-target boosting following secondary exposure to the antigen (Figure 2D).

V_H-dependent amplification of a serum antibody response targeting the Group 1 bnAb epitope

To appropriately activate and amplify the V_H-endowed antibody response, we reconfigured HA-np into an identical nanoparticle displaying the trimeric stalk-only domain of NC99 HA, termed SS-np (Yassine et al., 2015) (Figures 1D and 3A). Consistent with previous observations, this translated into an enhanced capacity to activate the germline-reverted CR6261 (gCR6261) BCR through its V_H gene-encoded CDRH2 contact to the stalk bnAb-epitope (Figure S3A and S3B).

We found that in contrast to HA-np, sequential immunization with SS-np now boosted antibodies to the Group 1 bnAb epitope, refocusing up to 50% of the serum antibody response upon this target (Figure 3A). In the control genotypes (not containing IGHV1-69), bnAb epitope-targeting was not observed in the serum response after sequential immunization with SS-np (Figure 3A). The magnitude of antigen specific IgG elicited by SS-np, as well as HA-np and NC99 virus, was nevertheless equivalent across all genotypes (Figure S4A). IGHV1-69-dependent antibody refocusing was also evidenced by logfold increases in serum neutralization activity against matched and unmatched H1N1 influenza strains (Figure 3B and S4B). This neutralization activity was lost when IGHV1-69 immune serum was pre-absorbed with HA but not with HAΔstem competitors, further indicating serum antibody refocusing to the Group 1 bnAb epitope (Figure 3B and S4B). By contrast, neutralization activity from the immune sera of the control genotypes were competed by HA and HAΔstem, indicating off-target polyclonal responses against the HA stalk.

Vaccine-amplification of human IGHV1-69 bnAb lineages

To isolate and characterize the IGHV1-69 BCRs expanded by SS-np, we performed H1-HA and H5-HA B cell probe staining and FACS on IgM and IgG B cell subsets throughout the SS-np immunization regimen. H1-and H5-HA dual probe reactivity was used to identify BCR affinity to the Group 1 bnAb-epitope as performed previously (Wheatley et al., 2015; Whittle et al., 2014). We found that dual-reactive B cells were not detected prior to immunization, indicating a low on-target precursor frequency, but were expanded following each exposure to SS-np (Figure 3C and S4C). Isolation and sequencing of the corresponding BCRs revealed selection for CDRH3 containing tyrosine at Kabat positions 98-100, motifs reproducibly observed in human IGHV1-69 bnAb lineages (Avnir et al., 2014; Lerner, 2011; Pappas et al., 2014; Wheatley et al., 2015; Whittle et al., 2014) (Figure 3D and 3E).

We observed SHM in CDRH1, CDRH2, and FR3 in the H1+ H5 reactive antibodies elicited by SS-np (Figure 4A and 4B). The elicited antibodies fell into three tiers following two or three exposures to SS-np: I) those that could neutralize across clinically relevant vaccine-unmatched Group 1 viruses (H1N1, H5N1, H9N2) with similar breadth as CR6261 (e.g. mAbs: S89, S53); II) those that neutralized two of the three subtypes (e.g. mAbs: S102), and III) those that only neutralized unmatched H1N1 (e.g. mAbs: S68, S49, S76) (Figure 4C and S4D–F). Affinity maturation of the SS-np induced mAbs averaged 6%, indicating that minimal SHM was needed to elicit this bnAb vaccine response (Figure 4D, S5A–C). Our Tier I antibodies were underscored by T28P, a well characterized ‘public’ mutation often conferring Group 1 neutralization breadth in IGHV1-69 bnAbs (Lingwood et al., 2012; Pappas et al., 2014). We did not detect any Group 2 neutralizing activity, consistent with the elicitation of a prototypic Group 1 IGHV1-69 bnAb response (Figure 4C and S4F). To confirm that the IGHV1-69 response was protective, we immunized IGHV1-69 and control C57Bl/6 mice with SS-np and then challenged with a subtype-unmatched avian H5N1 influenza virus (Figure 4E). Immunization of wildtype mice with SS-np has previously demonstrated protective efficacy against H5N1 avian challenge (Yassine et al., 2015), and in our animals, we found that vaccine protection was significantly elevated in the IGHV1-69 response ($P<0.05$, Mantel-Cox test of survivorship).

To define if this same response could be expanded in the presence of pre-existing immunity to influenza, mice were pre-infected with a sublethal dose of the unmatched H1N1 virus A/California/09/2009 (CA09), a major immunodominant target within human B cell memory (Guthmiller and Wilson, 2018; Raymond et al., 2018), and then sequentially immunized with SS-np (Figure 5A). After each immune challenge, we observed serum IgG refocusing to the Group 1 bnAb epitope in IGHV1-69 animals only, as measured by reactivity to HA and HAΔstem,derived from both NC99 and CA09 (Figure 5B). This refocusing was again underscored by expansion of human IGHV1-69 bnAb lineages, as indicated by expansion of Y98-100-containg BCRs (Figure 5C).

IGHV1-69 bnAb precursors in transgenic mice and human PBMC

Immunogenicity for a given antibody epitope can be controlled by the relative number of germline BCRs specific for that epitope (on-target BCRs) versus the number of germline BCRs specific for other competing epitopes (off-target BCRs) (Abbott et al., 2018; Dosenovic et al., 2018). Dual H1 and H5 staining of B cells from naïve IGHV1-69 animals indicated that despite V_H gene constrainment, the frequency of germline B cells specific for the Group 1 bnAb site was low and not well detected by this method (Figure 3C and S4C). To more accurately measure the frequency of germline BCRs specific for the bnAb epitope as displayed by our SS-np immunogen (on-target), versus those BCRs targeting non-bnAb sites on SS-np (off-target), we generated fluorescent SS-np B cell probes that discriminated between these antigenicities (Figure 6A and S6A–C). Two fluorescent versions of SS-np served as positive selectors (SS-np-A488 and SS-np-A594) and two fluorescent versions of SS-npΔstem (containing the I45R, T49R substitutions) served as negative selectors (SS-npΔstem-A546 and SS-npΔstem-A647) (Figure 6A and S6A–C). These probes were first validated for correct size and BCR antigenicity (Figure S6A–C) and then applied to interrogate our mouse and human B cell repertoires (Figure 6A–F and S6D). On-target IgM

BCRs were defined by reactivity to both SS-np labeled probes and not the SS-npΔstem probes, while off-target IgM BCRs were defined by reactivity to only the SS-npΔstem probes.

We found that the frequency of on-target IgM B cells was significantly elevated in IGHV1-69 animals, relative to control animal genotypes, which also held true when the frequency of on-target BCRs was normalized against the frequency of off-target BCRs (Figure 6C). In contrast to the control genotypes, the ratio of on-to-off target B cells in IGHV1-69 mice was > 1, indicating that V_H-endowed targeting conferred preferential specificity for the group 1 bnAb epitope (Figure 6C). The on-target IgM BCRs in IGHV1-69 animals also selected for CDRH3 sequences containing Y98-100, which were present in 45% of the on-target BCRs (Figure 6D). In human PBMC, the on-target IgM BCRs were biased for IGHV1-69 usage (comprising ~25% of the BCR sequences), of which 41% were enriched for Y98-100 (Figure 6E–F). The other on-target non-IGHV1-69 V_H genes did not select for tyrosine at this position (Figure 6F). The ratios of on-to-off-target germline B cells in humans vs IGHV1-69 mice were statistically indistinguishable (P>0.05, ANOVA) with on/off ratios >1 (Figure 6C and S6D).

Dilution of the IGHV1-69-endowed response to match the on-target frequency in human PBMC

B cell dilution experiments in the HIV vaccine space have been performed by adoptively transferring a near monoclonal source of CD45.2$^{+/+}$ B cells bearing a single VDJ constrained on-target BCR clone of interest into CD45.1$^{+/+}$ C57Bl/6 recipients (Abbott et al., 2018; Dosenovic et al., 2018). However, as our donor IGHV1-69 B cells were CDRH3 unconstrained (polyclonal), with an already diluted frequency of on-target B cells, further dilution by adoptive transfer would be hypophysiologic relative to the IGHV1-69 B cell frequency in humans (Figure S7A–C). Nevertheless, under these hypophysiologic conditions, we found that SS-np immunization of recipient CD45.1$^{+/+}$ mice enriched for IGHV1-69 bnAb precursors bearing Y98-100 in their CDRH3 within GCs (Figure S7D). These IGHV1-69 B cells were isolated by FACS using expression of GC markers, CD45.2, and co-reactivity for G6, a monoclonal anti-idiotypic antibody specific to the Phe54 position in the IGHV1-69 CDRH2 and has previously been deployed to measure IGHV1-69 usage in B cell responses to influenza vaccines (Avnir et al., 2016; Wheatley et al., 2015). All G6-reactive B cells were sequence verified as IGHV1-69, further confirming G6 specificity.

We then performed an *in vivo* IGHV1-69 B cell dilutions to encompass the human bnAb precursor frequency by breeding four transgenic mouse genotypes: IGHV1-69$^{+/+}$; IGHV1-69$^{+/-}$/C57Bl/6$^{+/-}$; IGHV1-69$^{+/-}$/IGHV1-2$^{+/-}$; and C57Bl/6$^{+/+}$ (Figure 7). Using IgM B cell reactivity to G6, we determined that all BCRs in the IGHV1-69$^{+/+}$ mice expressed IGHV1-69, while ~50% were IGHV1-69 in IGHV1-69$^{+/-}$/IGHV1-2$^{+/-}$ mice, and only ~3% were IGHV1-69 in the IGHV1-69$^{+/-}$/C57Bl/6$^{+/-}$ genotype (Figure 7A–C). The ~3% expression of IGHV1-69 in IGHV1-69$^{+/-}$/C57Bl/6$^{+/-}$ mice indicated a distinct preference for using native C57Bl/6 IgH instead of the engineered HC2 locus. Sequential (3x) immunization of these animals with SS-np elicited serum antibodies that were refocused upon the Group 1 bnAb epitope in direct proportion to the number of IGHV1-69

B cells present (Figure 7C and 7D). This occurred at all dilutions, both above and below the frequency of IGHV1-69 bnAb precursors as measured in human PBMC (Figure 7E).

Discussion

Antibody responses can show biased V_H gene usage, supporting the long-discussed notion that gene-encoded elements of the BCR harbor innate-like recognition characteristics that endow 'public' antigen targeting solutions (Casali and Notkins, 1989; Cohn and Langman, 1990; Henry Dunand and Wilson, 2015; Lerner, 2011; Lonberg, 2005; Pape et al., 2018; Schroeder et al., 1987). Here, we deployed purpose-built transgenic mice to experimentally evaluate the existence of gene-endowed epitope targeting as a function of immune challenge, and then assessed whether such public targeting provided a reproducible basis for vaccine-amplifying humoral responses against an otherwise immunologically subdominant site, namely the functionally conserved stalk bnAb epitope on Group 1 influenza viruses. We found that the human V_H gene IGHV1-69 endowed natural cognate specificity for this target and supported the elicitation of a low-threshold immunodominant bnAb response, which was activated and amplified using a single rationally designed immunogen. *In vivo* B cell dilution further demonstrated that this antibody focusing principle was dependent on the number of IGHV1-69 B cells present in repertoire and could be achieved when the precursor frequencies were within physiologic range. Collectively our results demonstrate that gene-endowed antibody targeting exists and could in principle be exploited to elicit bnAbs in humans.

Using reconstituted IGHV1-69 BCR-HA interactions, we found that CDRH2-input dominated over CDRH3-input in germline recognition of the Group 1 bnAb epitope, consistent with the V_H centric model of germline targeting to this site (Lingwood et al., 2012; Villar et al., 2016; Weaver et al., 2016) and the suggestion that IGHV1-69 usage may be deterministic for generating human influenza bnAb responses (Avnir et al., 2014; Lerner, 2011; Lingwood et al., 2012; Pappas et al., 2014; Sui et al., 2009; Weaver et al., 2016). To test this, we deployed humanized mice in which antibodies were fully constrained to single V_H genes of interest, but developed with unrestricted human CDRH3 diversity. Of the current single V_H gene knock-in mice, most are fixed to a single VDJ, while others are partially constrained to a select V_H gene with CDRH3 diversity arising from N-junctional diversification of murine D and J segments (Verkoczy et al., 2017) (see also Table S1). By contrast, complete V_H restriction in our system allowed for systematic evaluation of V_H contribution to epitope targeting in the serum antibody response, and in the context of human CDRH3 diversity. This is an important distinction, as CDRH3 is normally the principal determinant for antigen complementarity (Schroeder and Cavacini, 2010; Xu and Davis, 2000), and profoundly affects antibody targeting, as demonstrated in bovine humoral responses, wherein a baseline repertoire with longer CDRH3 sequences enables vaccine-elicitation of otherwise unattainable HIV bnAbs (Sok et al., 2017).

We found that exposure to NC99 H1N1 influenza virus elicited primary antibody responses engaging the Group 1 bnAb epitope, but only in IGHV1-69 animals. This experimentally demonstrates that IGHV1-69 endows for BCRs with natural specificity for the bnAb target as displayed by the native virus (Figure 2). Antibody subdominance to this epitope has been

thought related to inaccessibility arising from the dense packing of surface glycoproteins on the virion (Nabel and Fauci, 2010). However, our results show that IGHV1-69 endows on-target solutions that are insensitive to this parameter. Nevertheless, immunodistractive epitopes on the HA head domain are well established for sterically accessible HA trimer immunogens (Altman et al., 2015; Tan et al., 2019), and consistent with this, we found that bnAb-epitope specific B cells were outcompeted by off-target responses following secondary exposure to virus. Recapitulation of this viral immune-distraction effect by sequential immunization with the structurally defined HA-np (Kanekiyo et al., 2013) indicated that full length HA imposes an immunogenic structure that prevents productive expansion of IGHV1-69-endowed targeting of the Group 1 bnAb epitope. This was verified by sequential immunization with the homologous SS-np, which enabled IGHV1-69-dependent refocusing of ~50% of the serum antibody response upon the bnAb target.

The inability of SS-np to elicit IgG against the Group 1 bnAb-epitope in the control genotypes illustrates an important vaccine principle, namely that optimized display of the target does not circumvent immunological subdominance if the baseline CDRH3 repertoire is unable to reproducibly engage the epitope of interest. However, we found that if the same CDRH3 repertoire was coupled to a gene-endowed antibody affinity for the target, then a genetically reproducible basis for engagement was present, allowing for pathway-based amplification of the bnAb response. Along this line, the titer of antibodies engaging a given epitope can be controlled by the relative number of on-target versus off-target BCRs present in the germline B cell repertoire (Abbott et al., 2018; Dosenovic et al., 2018). The reason SS-np elicited bnAbs in IGHV1-69 animals and not control genotypes was because IGHV1-69 usage selectively increased the frequency of on-target germline BCRs specific for the Group 1 bnAb epitope as displayed by SS-np relative to the frequency of off-target BCRs specific for non-bnAb sites on this immunogen. By contrast, within the control genotypes, germline BCRs specific for non-bnAb sites on SS-np were numerically superior to those specific for the bnAb epitope. Importantly, the proportion of CDRH3 bearing Y98-100, a non-obligate but reproducible marker of IGHV1-69 bnAb lineages (Avnir et al., 2014; Lerner, 2011; Pappas et al., 2014; Wheatley et al., 2015; Whittle et al., 2014), was comparable across all genotypes, indicating that IGHV1-69 constrainment did not skew the repertoire toward potentially favorable CDRH3 sequences. Rather it was the genetic insertion of IGHV1-69 encoded CDRs that now made favorable the elicitation of a serum antibody response refocused upon the Group 1 bnAb epitope.

The hydrophobic CDRH2 encoded by IGHV1-69 has long been proposed to provide multiple non-overlapping/polyreactive antigen specificities (Andrews et al., 2015; Casali and Notkins, 1989; Kipps et al., 1990; Lerner, 2011). Our results indicate that when SS-np is the antigen, such activity becomes preferentially focused on the Group 1 bnAb epitope. Importantly, repertoire constrainment to IGHV1-69 did not alter B cell numbers or development *in vivo,* as might be expected if this V_H gene was deterministic for generating autoreactive B cells.

Critically, pre-immunity to an unmatched CA09 influenza virus, a strain that currently dominates influenza B cell memory in humans (Guthmiller and Wilson, 2018; Raymond et al., 2018), did not prevent IGHV1-69 dependent refocusing to the bnAb epitope following

immunization with SS-np; rather it primed antibody responses against this site. On-target priming by diverse H1N1 viruses further underscores the broad immunoreceptor activity of IGHV1-69-encoded CDRs for the Group 1 bnAb site and suggests that the corresponding bnAb response is able to 'resist' some potentially confounding aspects of immune history, a key requirement for universal vaccination (Erbelding et al., 2018).

In all cases antibody refocusing to the Group 1 bnAb epitope was underscored by vaccine-amplification of human IGHV1-69 bnAb lineages, both in naïve animals and those with established H1N1 immune history. This was evidenced by expansion of BCRs bearing Y98-100 in CDRH3 resulting in the elicitation of pan-Group 1 bnAbs, with the greatest neutralizing breath yet achieved in an animal influenza vaccine model. This response was low threshold as bnAbs could be induced after only two exposures to SS-np, and only required an average of 6% affinity maturation to achieve panGroup 1 neutralization activity, a value lower than the ~15% SHM typically seen in human IGHV1-69 bnAbs (Avnir et al., 2014; Lerner, 2011; Pappas et al., 2014; Whittle et al., 2014). SHM was also almost exclusively concentrated in the HC, as would be expected for IGHV1-69 bnAbs, where LC contact is not indispensable but is minimal for this antibody class (Lingwood et al., 2012; Pappas et al., 2014). Neutralization activity in the SS-np-elicited responses was also underscored by T28P, a reproduced/public mutation often deployed in humans to confer IGHV1-69 Group 1 neutralization breadth (Lingwood et al., 2012; Pappas et al., 2014). Elevated affinity maturation was expected postboost 2, however recent data suggests that IgG B cell memory does not necessarily re-seed GCs following repeat antigen exposure (Shlomchik, 2018) and therefore may not accumulate mutations, at least in mice. While this remains debated (Pape and Jenkins, 2018), the important pre-clinical message is that human IGHV1-69 bnAb responses have a minimalist affinity maturation requirement that can be met by a single influenza immunogen that broadly stimulates on-target germline precursors through a natural V_H 'encoded' affinity for cognate antigen. This contrasts the challenge for vaccine-elicitation of V_H-constrained HIV bnAbs, where although effective germline priming has been achieved in some animal models (Table S1), an unknown number of stain-variant 'shepherding' immunogens are likely needed to sequentially boost the response to attain the exceptional SHM needed for HIV neutralization breadth (Peterhoff and Wagner, 2017; Verkoczy et al., 2017).

SS-np may also be capable of eliciting this same low-threshold bnAb response from the human B cell repertoire. We found that within human PBMC there was a greater frequency of germline IgM BCRs specific for the bnAb epitope than those specific for non-bnAb sites on SS-np. Furthermore, IGHV1-69 B cells using Y98-100 accounted for a substantial fraction of these on-target BCRs. IGHV1-69 also displays allelic polymorphism in CDRH2 (F54 vs L54 variants), where the F54 alleles (homozygous in both our IGHV1-69 mice and in the patients sequenced) are generally more common and supply the prototypic IGHV1-69 bnAb response (Avnir et al., 2014; Avnir et al., 2016; Lingwood et al., 2012; Pappas et al., 2014; Wheatley et al., 2015). Importantly, our B cell dilution experiments demonstrated that SS-np can selectively prime IGHV1-69 bnAb precursors when present at hypo-physiologic cell numbers and can refocus the serum antibody response upon the bnAb-epitope when these precursors were present at physiologic frequencies. This refocusing was also dose-dependent and was directly proportional to the number of IGHV1-69 B cells present in the

repertoire, again underscoring a gene-hardwired and vaccine-expandable pathway that SS-np appears poised to elicit in humans. Studies of early human fetal B cell repertoire have demonstrated enriched usage of F54 IGHV1-69 (up to 14% of BCRs) (Schroeder et al., 1987), suggesting that SS-np could be particularly effective in eliciting the response within infants and young children.

The influenza bnAb elicitation principle we describe in this study demonstrates that usage of certain human antibody gene-encoded CDRs causally and broadly endow for rapid, low threshold vaccine-amplifiable antibody responses targeting an otherwise immunologically subdominant but ‘universal’ vaccine target on influenza virus. This antibody-focusing principle may also be applicable for amplifying other bnAb responses, such as V_H gene restricted bnAb development pathways that neutralize Group 1 and Group 2 influenza viruses (Joyce et al., 2016).

STAR METHODS

LEAD CONTACT AND MATERIALS AVAILABILITY

Further information and requests for reagents should be directed to and will be fulfilled by the Lead Contact, Daniel Lingwood (dlingwood@mgh.harvard.edu). There are restrictions to the availability of the IGHV1-69 and IGHV1-2 transgenic mice due to a MTA with Bristol-Myers Squibb.

EXPERIMENTAL MODEL AND SUBJECT DETAILS

Mice—The mice used in these studies were developed using a pre-established strategy that fully constrains V_H usage to user-defined gene segments, while allowing for normal and random recombination with diverse human D and J segments (Fishwild et al., 1996; Lonberg et al., 1994). Thus, B-cell rearrangements that underlie variable region generation in these mice fully fixes to CDRH1 and CDRH2 domain usage while allowing for normal CDRH3 formation. Successfully recombined antibody segments are substrates for subsequent affinity maturation. The variable region domain as found in the HC2 human-Ig construct (Fishwild et al., 1996; Lonberg et al., 1994; US patent US6255458B1) was used as the starting substrate for plasmid recombineering (Gene Bridges, GmBH). Briefly, the four original V_H segments present in HC2 were removed, and replaced by single synthetic DNA constructs corresponding to individual V_H segments. This modular cassette system was developed to enable delivery of functional, unmodified single genomic V_H domains comprising V_H coding regions and endogenous regulatory and recombination signals into the V_H-deleted HC2 variable region recipient. As reported here, synthetic genomic DNA constructs of ~6.6kb derived from human V_H alleles IGHV1-69*01 or IGHV1-2*02 were synthesized at Geneart (Regensburg, Germany) using coding sequences obtained from IMGT “IG and TR” Repertoire (http://www.imgt.org/). Specific coordinates of synthesized DNA fragments correspond to NCBI’s GRCh38.p12 Primary Assembly of huChr14 (nts 106720648-106714041 for IGH1-69*01 and nts 10599108-105984851 for IGHV1-2*02). Transgenic animals were generated per standard techniques (Pease, Shirley, and Thomas L. Saunders. Advanced Protocols for Animal Transgenesis: an ISTT Manual. Springer, 2011) and were a gift to D.L. from Bristol-Myers Squibb (Redwood City, CA). The transgenic

mice used in this study (IGHV1-69*01 animals and IGHV1-2*02) consisted of the following genotypes: IGHV1-69$^{+/+}$; IGHV1-2$^{+/+}$; IGHV1-69$^{+/-}$IGHV1-2$^{+/-}$; IGHV1-69$^{+/-}$C57Bl/6$^{+/-}$, and all were wild-type C57Bl/6 for light chain expression.

Animals were maintained within Ragon Institute's HPPF barrier facility and all experiments were conducted with institutional IACUC approval (MGH protocol 2014N000252). **In this study, both male and female animals, aged 6-10 weeks, were used.**

Human PBMC—Human PBMC were isolated from Leukopacs obtained from the MGH blood donor center (9 patients). Prior to donating blood donation, the human subjects were required to sign a donor attestation/consent statement, as per hospital requirements. It states: "I give permission for my blood to be used for transfusion to patients or for research". The gender as well as the age/developmental stage of the patients is not recorded by the MGH blood donor center, however eligible donors must be a minimum of 16 years of age and weigh a minimum of 110lbs. All experiments with human PBMC were conducted with institutional IBC approval (MGH protocol 2014B000035).

METHODS DETAILS

Recombinant immunogens and B cell probes—HA ectodomains from A/New Caledonia/20/1999 (NC99) or A/California/04/2009 (CA09) were expressed in and purified from 293F cells as soluble wildtype and HAΔstem (I45R, T49R) trimers, or as NC99 ferritin nanoparticles displaying 8 copies of either full length HA trimer (HA-np) or stalk-only trimer (SS-np), as performed previously (Kanekiyo et al.; Weaver et al., 2016; Yassine et al., 2015). Briefly, 293F cells grown in Freestyle media were transfected with 500 μg/L of HA or probe plasmid (293fectin™ Reagent). At day five, the culture supernatant was collected, filtered and loaded on either Ni Sepharose resin (GE Healthcare) for HA trimers, or Erythrina cristagalli Gel-ECA-Immobilized Lectin (EY Laboratories) for HA-np and SS-np by gravity flow. For purification of HA trimer, the resin was further washed with 20mM imidazole and eluted in 500mM imidazole. For purification of HA nanoparticles, the resin was washed in PBS and eluted in 0.2M lactose. All proteins were then separated by size exclusion chromatography (SEC) using an AKTA pure protein purification system (GE Healthcare). A Superdex 200 10/300 column was used to purify HA trimers while the Superose 6 10/300 column was used for HA nanoparticles.

For B cell probes, Y98F versions of soluble trimeric HA ectodomains from NC99 (H1) and A/Indonesia/05/2005 (H5) were also generated and purified as described above (Wheatley et al., 2015; Whittle et al., 2014). Y98F is a mutation that prevents surface sialic acid binding (Whittle et al., 2014). The H1/H5 probes also contained an Avi-Tag, which was biotinylated and labeled with streptavidin-phycoerythrin (H1-PE) or streptavidin-allophycocyanin (H5-APC), producing fluorescent tetramers of HA trimers (Weaver et al., 2016; Whittle et al., 2014). The SS-np probes were fluorescently labeled with Alexa 488 and Alexa 594, and the SS-npΔstem (I45R, T49R) probes were fluorescently labeled with Alexa 647 and Alexa 546 and then re-purified by SEC. All recombinant HA proteins were quality controlled by SEC and by binding to the conformational antibodies CR6261 and CH65 (Whittle et al., 2014; Yassine et al., 2015). The G6 antibody was a gift from Dr. Roy Jeffris (University of

Birmingham, U.K.). G6 was labeled with either Alexa 647 or Pacific Blue using commercial conjugation kits.

Reconstituted BCR – antigen interactions—Unmutated germline revertants of *IGHV1-69*-derived bnAbs were expressed as mIgM in 293F cells (Lingwood et al., 2012; Weaver et al., 2016). Two days post-transfection, 2×10^6 cells expressing germline membrane IgM versions of CR6261, FE53, 1009-3B05 with mutations in CDRH2 or CDRH3, or VRC01 (isotype control) were placed on ice, incubated with violet fluorescent reactive dye, washed and then incubated for 1 hr at 4°C in PBS containing 1% FBS with either 0.4μg PE-HA, 0.4μg PE-HAΔstem, or PE mouse anti-human lambda chain (BD Biosciences) to confirm surface trafficking of CR6261 germline mIgM, or PE-anti-human kappa chain (eBioscience) to confirm surface trafficking of FE53 and 1009-3B05 germline mIgMs. Cells were washed twice and then fixed in 0.5% PFA in PBS. PE surface intensity from Violet-negative singlet 293F cells was measured by flow cytometry.

***In vitro* Germline BCR triggering—**The capacity of SS-np vs HA-np preparations to trigger gCR6261 BCR signaling was evaluated through activation of Ramos cells engineered to display mono-specific IgM BCRs of interest, as previously described (Villar et al., 2016; Weaver et al., 2016; Yassine et al., 2015). Briefly, 1×10^6 B cells displaying gCR6261 BCR or its variant containing a CDRH2 binding mutant (I53A, F54A) (Lingwood et al., 2012; Weaver et al., 2016) were exposed to 0.5 μM SS-np; 2.5pM HA-np; 5 μM of HA trimer; or 0.5 μg/μl mouse anti-human IgM $F(ab')_2$ (Southern Biotech). HA-np and HA trimer were engineered with the Y98F mutation to prevent superantigen-like BCR stimulation by HA lectin activity (Villar et al., 2016). BCR stimulation was measured by flow cytometry (LSR II, BD Immunocytometry Systems) as the ratio of the Ca^{2+} bound/unbound states of the dye Fura Red and ratiometric measures for individual cells were normalized to total Ca^{2+} flux as measured by exposure of cells to 10 μg/ml ionomycin.

Immune challenges—Mice were bled prior to all experiments. For NC99 infection, mice were sequentially infected intranasally at week 0, 3, and 6 with $10^{5.4}$ $TCID_{50}$ units/ml of virus, a previously established sublethal dose for this influenza strain (Glaser et al., 2007). Blood was collected 14 days after each infection time point. For protein antigens, each mouse genotype was immunized with 15ug of SS-np or equimolar HA-np in a 100ul inoculum containing 50% w/v Sigma adjuvant, as described previously (Kanekiyo et al.; Yassine et al., 2015). Akin to the viral infection regimen, intraperitoneal immunizations were performed sequentially at weeks 0, 3 and 6, with blood collected two weeks after each inoculation. For some experiments, pre-existing H1N1 immunity was established by pre-infecting with a sublethal dose of CA09 ($10^{5.8}$ $TCID_{50}$/ml) at week 0 followed by sequential immunization with SS-np at weeks 3 and 6. To assess vaccine-protection, the SS-np immunization regimen was repeated in each animal genotype (n=5 per group) and then followed by an intranasal challenge with$10^{6.4}$ TCID50 units/ml of a low path H5N1 avian influenza (A/chicken/Viet/NCVD-016/2008/(H5N1)-PR8-IDCDCRG12) at week 8 (two weeks after the final SS-np immunization). Survivorship over the next ten days was evaluated and animals that lost 15% of the initial body weight during this period were humanely euthanized. This endpoint was expressly enforced by our Institutional Animal

Care Committee. The H5 ressortant virus was produced using plasmid-based reverse genetics (Neumann et al., 1999) and contains 6 internal genes from A/Puerto Rico/8/1934 (H1N1) with HA and NA genes derived from those of the parental virus [A/chicken/Vietnam/NCVD-016/2008 (H5N1) (USDA permit#133390). Seed stocks for all the viruses used in this study were obtained from the Centers for Disease Control and Prevention International Reagent Resource (IRR - Atlanta, Georgia, USA) and were grown in ten day-old embryonated chicken eggs or in Madin-Darby canine kidney (MDCK) cells.

ELISA

Protein antigens (HA, HAΔstem, SS-np and HA-np) were coated onto 96 well Nunc MaxiSorp plates at 200ng HA per well. The plates were blocked with 2% BSA in PBS for 1 hour and washed with PBS and 0.05% Tween 20 (PBST). After blocking, mAbs or immune sera was added and incubated for 1 hour. To assess serum antibody responses, samples were initially diluted at 1:20 followed by 1:5 serial dilutions in PBS. Monoclonal antibodies were tested at 10ug/ml and further diluted 1:5 in PBS. Plates were washed with PBST and incubated with sheep anti-mouse IgG-HRP (GE Healthcare) or sheep anti-human IgG-HRP (GE Healthcare) at 1:5000 dilution in PBS. Plates were developed using TMB substrate, quenched with 1N sulphuric acid, and then read at 450nm using the Teacan Infinite m1000 Pro microplate absorbance reader (Männedorf, Switzerland). Loading of HA and HAΔstem (NC99 versions) was standardized by reactivity to CH65, an RBS-specific mAb. For CA09 versions of HA and HAΔstem, loading was standardized by anti-his tag reactivity. To quantify mAb or serum IgG reactivity to HA vs HAΔstem, area under the curve was calculated using GraphPad PRISM software. These values were then evaluated using a method for comparing two under the curve areas (Hanley and McNeil, 1983), which tests the two sided null hypothesis that the distribution of Z is centered on zero ($P>0.05$) and includes correction for curves derived from the same subject.

Flow Cytometry and B-cell Sorting—B cell and T cell phenotypes in the spleens of IGHV1-69, IGHV1-2 and wildtype C57Bl/6 mice were assessed using a cocktail of mouse specific B cell- and T cell-specific flow cytometry antibodies: CD4 Alexa Fluor 700 (BD Biosciences); and CD3e PE-Cy7 (Biolegend), CD19 BV421 (BioLegend), IgM BV605 (BioLegend), IgG PerCPCy5.5 (Biolegend). Single cells suspensions were obtained using a 70gm cell strainer and treated with ACK lysis buffer. The cells were washed in PBS and then stained with Aqua Live/Dead amine-reactive dye (0.025 mg/ml) before the B cell and T cell staining panel was applied. To isolate SS-np-elicited B cells, mouse spleens were stained as above, with the addition of 0.25gg of H1-PE and H5-APC probes, as previously described (Weaver et al., 2016; Whittle et al., 2014). Single cells ($CD3^-/CD19^+/IgG^+/IgM/H1^+/H5^+$) were sorted into 96 well plates containing RLT lysis buffer supplemented with 1% beta-mercaptoethanol (BME). In unimmunized IGHV1-69 and IGHV1-2 animals, antigen naïve B cells ($CD3^-/CD19^+/IgG^-/IgM^+$) were also bulk sorted into RLT lysis buffer with 1% BME. In all cases, the cells were immediately frozen and stored at $-80^{\circ}C$ for subsequent analysis. The same staining procedure was applied to the splenocytes of unimmunized IGHV1-69 animals and H1+H5 cross-reactivity was measured in the $CD19^+/IgG^+/IgM^-$ and CD $19^+/IgG^-/IgM+$ sub sets.

When applying SS-np B cell probes, the fluorescent SS-np and SS-npΔstem probes were first tittered against human BCR reporter cell lines expressing either FE53 IgM BCR or control VRC01 IgM BCR, as previously described (Weaver et al., 2016). Briefly, cells were placed on ice, incubated with violet fluorescent reactive dye, washed and then incubated for 1 hr at 4°C in PBS containing one of each of the four fluorescently labeled SS-np probes (0.25 μg of SS-np-Alexa 488, SS-np-Alexa 594, SSΔstem-np Alexa 647, or SSΔstem-np Alexa 546). The cells were then washed twice, resuspended in PBS and analyzed on a 5 Laser LSR Fortessa (BD Biosciences). To determine the frequency of on-target and off-target germline IgM B cells, mouse spleens were processed and stained with the T and B cell staining panel as above but now containing 0.25μg each of SS-np Alexa 488, SS-np Alexa 594, SS-npΔstem Alexa 647, and SS-npΔstem Alexa 546. 2-5 million events were recorded using the FACS Aria Fusion Sorter (BD Biosciences). On-target germline B cells were defined as CD3^{-}/CD19+/IgM+/IgG^{-}/SS-np Alexa 488+/SS-np Alexa 594+/SS-npΔstem Alexa 6477SS-npAstem Alexa 546'. Off-target germline B cells were defined as CD3^{-}/CD19+/IgM+/IgG^{-}/SS-np Alexa 488^{-}/SS-np Alexa 5947SSAstem-np Alexa 647+/SS-npΔstem Alexa 546+. Individual on-target B cells were sorted into 96 well plates containing RLT lysis buffer supplemented with 1% BME.

For human PBMC (Patients 1-9), the cells were stained with Aqua Live/Dead amine-reactive dye, washed, and incubated with a cocktail of B cell and T cell-specific flow cytometry antibodies: CD19 Alexa 700 (Biolegend), IgG BV421 (BD Biosciences), IgD PE-Cy7 (BD Biosciences), IgM PerCP-Cy5.5 (BioLegend), CD3 APC-Cy7 (BD Biosciences); and 0.25μg each of SS-np Alexa 488, SS-np Alexa 594, SS-npΔstem Alexa 647 and SS-npΔstem Alexa 546. On-target and off-target B cells were defined as stated above. Individual on-target cells were isolated by FACS in Patients 1-3 who were homozygous for the F54 containing CDRH2 alleles of IGHV1-69 and processed for BCR sequencing. Downstream analyses of the data were performed using FlowJo software version 9.3.2 (TreeStar).

B cell dilution experiments—B cell adoptive transfer experiments were performed as described previously (Abbott et al., 2018; Dosenovic et al., 2018). Briefly, resting antigen naïve IgM B cells were purified from our CD45.2$^{+/+}$ IGHV1-69 mice using a MACS cell separation kit and transferred to recipient CD45.1$^{+/+}$ C57Bl/6 mice by intravenous injection. Twenty-four hours later, the recipient mice were primed with 100ug of SS-np, injected intraperitoneally. Eight days later, spleens were processed as mentioned above and stained with a cocktail of the following antibodies: CD4, CD8a – APCe780 (Thermofisher); B220 BV605 (BioLegend); GL7 Alexa 488 (BioLegend); CD95 PE/Cy7 (BD Biosciences); CD45.1 PerCP/Cy5.5 (BioLegend); CD45.2 PE (BioLegend); G6 Alexa 647 (0.25μg). IGHV1-69 B cells that participated in the subsequent germinal center reaction were defined as CD3^{-}/CD4^{-}/B220^{+}/GL7^{+}/CD45.1^{-}/CD45.2^{+}/G6^{+}, and were individually sorted by FACS into 96 well plates containing RLT lysis buffer supplemented with 1% BME. G6 is a monoclonal anti-idiotypic antibody specific to the Phe54 position in the IGHV1-69 CDRH2 and has been previously deployed to measure IGHV1-69 usage in B cell responses to influenza vaccines (Avnir et al., 2016; Wheatley et al., 2015).

B cell dilutions were also achieved genetically by generating the following genotypes: IGHV1-69$^{+/+}$, IGHV1-2$^{+/+}$, IGHV1−69$^{+/−}$/IGHV1-2$^{+/−}$; IGHV1-69$^{+/−}$C57Bl/6$^{+/−}$ The

proportion of IGHV1-69 B cells in each genotype was measured as $CD3^{-}$/$CD4^{-}$/CD19+/IgM+/G6+. As G6 binds specifically to the CDRH2 of IGHV1-69 antibodies (Avnir et al., 2017), the germline-endowed paratope for recognizing the Group 1 bnAb epitope, we found that it competed for recognition using our four-color SS-np/SSΔstem-np approach previously used to measure the fraction of on/off-target IGHV1-69 IgM B cells. Consequently, we estimated these values by multiplying the proportion of G6 positive $CD19^{+}$/IgM^{+} splenocytes in each genotype by the measured fraction of on-target B cells in animals fully constrained to IGHV1-69 (IGHV1-$69^{+/+}$ genotype). To obtain the corresponding frequencies of Y98-100 usage in these genotypes, these values were multiplied by 0.45, the measured proportion of CDRH3 bearing Y98-100 in the on-target IgM BCRs of IGHV1-$69^{+/+}$ animals. The proportion of CDRH3 bearing Y98-100 in the on-target IGHV1-69 IgM BCRs of human PBMC was 0.41. Each animal genotype (IGHV1-$69^{+/+}$; IGHV1-$2^{+/+}$; IGHV1-$69^{+/-}$IGHV1-$2^{+/-}$; IGHV1-$69^{+/-}$C57Bl/$6^{+/-}$) was then subjected to our 3x sequential immunization regimen using SS-np.

BCR sequencing—We enriched BCR libraries from single-cell (H1 + H5 reactive; SS-np/SSΔstem-np sorted; germinal center sorted) whole transcriptome amplification (WTA) products that were generated using the Smart-Seq2 protocol (Trombetta et al., 2014). To enrich BCR sequences from WTA after two 0.8x (v/v) SPRI bead-based cleanups and cDNA quantitation/normalization, we amplified both the heavy and light chain of each single cell (FR1 to CDR3) separately (HotStarTaq Plus), using a pool of partially degenerate V region specific gene primers against all possible IGHV (human) or IGLV (mouse) and IGKV (mouse) segments in the FR1 region (final concentration: 0.5 μM each) and reverse primers against the heavy or light constant regions (final concentration: 1μM each) (Scheid et al., 2009; Tiller et al., 2009) attached to the Illumina P7 (V region) and P5 (constant region) sequences (see Table S2). Following BCR amplification, a 0.8x (v/v) SPRI cleanup was performed, and amplicons were quantified and normalized to 0.2-0.5 ng/μL Using a step-out PCR (Kapa HiFi HotStart ReadyMix), we next added cellular barcodes and Illumina sequencing adapters (based on Nextera XT Index Adapters, Illumina Inc.) to each amplified heavy and light chain. Following purification with a 0.8x (v/v) SPRI and sample pooling, the paired heavy and light chain single-cell BCR libraries were sequenced using paired end 250×250 reads and 8×8 index reads on an Illumina MiSeq System. After demultiplexing, we paired heavy and light chain reads, reconstructed overlapping sequencing reads (PandaSeq, (Masella et al., 2012)), and aligned against the human IMGT database (Shi et al., 2014) with PCR/sequencing error correction using MigMAP, a wrapper for IgBlast (https://github.com/mikessh/migmap). Finally, consensus V-chain and L/K-chain for each single cell were determined by collapsing all reads with the same CDR3 sequence and calling the top heavy and light chain sequences by frequency. Any heavy or light sequence without at least 25 reads or frequency two-times greater than the next sequence of the same chain was denoted as without consensus.

The BCRs from antigen naïve IgM B cells ($CD3^{-}$/$CD19^{+}$/IgG^{-}/IgM^{+}) were also sequenced in bulk to evaluate CDRH3 diversity in IGHV1-69 and IGHV1-2 animals (>5 million BCR reads). For this, we performed the same WTA step using the Smart-Seq2 protocol (Trombetta et al., 2014) and the two subsequent PCR steps as above, except that in the first

PCR, the cocktail of V gene primers was replaced with a forward primer specific for the FR3 region within the V_H gene of interest (IGHV1-69 or IGHV1-2; see Table S2). We then sequenced the resulting product (FR3 to CDRH3) on an Illumina MiSeq, as above except without index reads, and aligned the resulting paired end FASTQs using MIXCR (Fahnrich et al., 2017). We used the following parameter in the alignment step of MIXCR: OvParameters.geneFeatureToAlign = {FR3Begin:Vend}, and restricted alignment to only heavy chain matches. Any reads with low sequence quality were trimmed by MIXCR using the default settings. To define the corresponding CDRH3 diversity in the human repertoire, we mined data from a recent study of naïve B-cell receptor ($CD3^-/CD19^+/IgM^+/IgG^-$) sequences (DeWitt et al., 2016), specifically the naïve B cell sequences from Donor 3. Using tcR (Nazarov et al., 2015) and custom scripts, we parsed the sequenced IGHV1-69 and IGHV1-2 naïve IgM B cells and the mined human data to generate frequency plots of CDRH3 length and assigned Kabat numbering for amino acid composition of 15aa and 16aa length CDRH3s. After filtering, we compiled the following total number of reads: IGHV1-69 – $6.66*10^6$; IGHV1-2 – $5.72*10^6$; human – $55.1*10^6$. The ranges of CDRH3 sizes for each sample were the following: IGHV1-69 – 4-35aa; IGHV1-2 – 4-36aa; human – 3-39aa. CDRH3 sequence logos were made by WebLogo (https://weblogo.berkeley.edu) as described previously (Crooks et al., 2004).

The proportion of CDRH3 containing Y98-100 within the IgM B cell repertoires were calculated for the IGHV1-69 and IGHV1-2 mice, humans (Donor 3) (DeWitt et al., 2016), and also for wildtype C57Bl/6 mice by mining a recent IgM BCR repertoire analysis (Rettig et al., 2018).

Production of Monoclonal Antibodies—The variable sequences from BCR heavy chains (HC) and light chains (LC) were synthesized as gene blocks (GenScript) and then cloned into human IgG HC and LC expression plasmids for transfection using our 293F protein production platform (Villar et al., 2016; Weaver et al., 2016). Monoclonal antibodies, including human bnAb IgG standards (CR6261, gCR6261, CH65, VRC01) were expressed as described above, with the exception that expression was for 6 days and the culture supernatant was passed over Protein G Sepharose. The column was washed in PBS, and then eluted in IgG elution buffer into 1M Tris, pH 8. The eluted IgG were further purified by SEC using a Superdex 200 10/300 column on the AKTA FPLC system (GE Healthcare).

Pseudotyped Neutralization Assays—*In vitro* neutralization assays were conducted in 293A cells using luciferase encoding lentiviruses pseudotyped for influenza HA and NA, as described previously (Kong et al., 2006; Yang et al., 2007). HA and NA sequences used to generate pseudoviruses were derived from: Group 1 [A/New Caledonia/20/1999 (H1N1), A/Singapore/6/1986 (H1N1), A/Vietnam/1203/04 (H5N1), A/Hong Kong/1073/99 (H9N2)] and Group 2 viruses [A/Hong Kong/1/1968 (H3N2), and A/Anhui/1/2013 (H7N9)]. Briefly, mouse sera were treated with receptor destroying enzyme (RDE) and heat-inactivated before use in neutralization assays. Immune sera or monoclonal antibodies were serially diluted and incubated with pre-titrated HA-NA pseudotyped viruses before addition to 293A cells. For competition assays, mouse immune sera were pre-incubated with HA, HAΔstem, or control RSV F protein (at a final concentration of 50 μg/ml) prior to measuring neutralization

activity against the above pseudoviruses. IC_{50} values were calculated from neutralization curves generated by GraphPad Prism software (v7.0).

Quantification and Statistical Analysis

All statistical analysis was performed using Prism Graphpad software. Sample sizes of animals and specific tests to determine statistical significance used are indicated in the methods and corresponding figure legends. Data were considered statistically significant at *p<0.05, **p<0.01, ***p<0.001, ****p<0.0001.

DATA AND CODE AVAILABILITY

Single cell and bulk sequencing data from IGHV1-69 and IGHV1-2 mice as reported in this publication have been deposited in NCBI's Gene Expression Omnibus and are accessible through GEO accession number GSE135761 (https://www.ncbi.nlm.nih.gov/geo/query/acc.cgi?acc=GSE135761).

Supplementary Material

Refer to Web version on PubMed Central for supplementary material.

Acknowledgments

D.L. was supported by NIH grants (R01AI137057-01, DP2DA042422, R01AI124378), the Harvard University Milton Award, The Gilead Research Scholars Program and Strategic Initiatives and Sundry funding from the Ragon Institute. M.S. and S.W.K. were supported by the NSF Graduate Research Fellowship Program. A.K.S. was supported by the Searle Scholars Program, the Beckman Young Investigator Program, the Pew-Stewart Scholars, a Sloan Fellowship in Chemistry, NIH grants 1DP2OD020839, 2U19AI089992, 1U54CA217377, P01AI039671, 5U24AI118672, 2RM1HG006193, 1R33CA202820, 2R01HL095791, 1R01AI138546, 1R01HL126554, 1R01DA046277, 2R01HL095791, and Bill and Melinda Gates Foundation grants OPP1139972 and BMGF OPP1116944. Support was also provided by the Ragon Institute NIH-funded Centers for AIDS Research (P30 AI060354, Harvard University Center for AIDS Research), supported by NIH co-funding and participating Institutes and Centers: NIAID, NCI, NICHD, NHLBI, NIDA, NIMH, NIA, FIC, and OAR. We thank BMS for gifting transgenic mice to D.L. and Roy Jeffris for providing the G6 antibody. We also thank Facundo Batista for helpful discussion and Celina Keating, Thalia Bracamonte Moreno, Vintus Okonkwo, and Matthew Smoot for recombinant protein production and the MGH Center for Comparative Medicine for their help with animal experiments.

References

Abbott RK, Lee JH, Menis S, Skog P, Rossi M, Ota T, Kulp DW, Bhullar D, Kalyuzhniy O, Havenar-Daughton C, et al. (2018). Precursor Frequency and Affinity Determine B Cell Competitive Fitness in Germinal Centers, Tested with Germline-Targeting HIV Vaccine Immunogens. Immunity 48, 133–146 e136. [PubMed: 29287996]

Altman MO, Bennink JR, Yewdell JW, and Herrin BR (2015). Lamprey VLRB response to influenza virus supports universal rules of immunogenicity and antigenicity. Elife 4.

Andrews SF, Huang Y, Kaur K, Popova LI, Ho IY, Pauli NT, Henry Dunand CJ, Taylor WM, Lim S, Huang M, et al. (2015). Immune history profoundly affects broadly protective B cell responses to influenza. Science translational medicine 7, 316ra192.

Angeletti D, Gibbs JS, Angel M, Kosik I, Hickman HD, Frank GM, Das SR, Wheatley AK, Prabhakaran M, Leggat DJ, et al. (2017). Defining B cell immunodominance to viruses. Nature immunology 18, 456–463. [PubMed: 28192417]

Avnir Y, Tallarico AS, Zhu Q, Bennett AS, Connelly G, Sheehan J, Sui J, Fahmy A, Huang CY, Cadwell G, et al. (2014). Molecular signatures of hemagglutinin stem-directed heterosubtypic

human neutralizing antibodies against influenza A viruses. PLoS pathogens 10, e1004103. [PubMed: 24788925]

Avnir Y, Watson CT, Glanville J, Peterson EC, Tallarico AS, Bennett AS, Qin K, Fu Y, Huang CY, Beigel JH, et al. (2016). IGHV1-69 polymorphism modulates anti-influenza antibody repertoires, correlates with IGHV utilization shifts and varies by ethnicity. Scientific reports 6, 20842. [PubMed: 26880249]

Avnir Y, Prachanronarong KL, Zhang Z, Hou S, Peterson EC, Sui J, Zayed H, Kurella VB, McGuire AT, Stamatatos L, et al. (2017). Structural Determination of the Broadly Reactive Anti-IGHV1-69 Anti-idiotypic Antibody G6 and Its Idiotope. Cell Rep 21, 3243–3255. [PubMed: 29241550]

Bonsignori M, Scott E, Wiehe K, Easterhoff D, Alam SM, Hwang KK, Cooper M, Xia SM, Zhang R, Montefiori DC, et al. (2018). Inference of the HIV-1 VRC01 Antibody Lineage Unmutated Common Ancestor Reveals Alternative Pathways to Overcome a Key Glycan Barrier. Immunity 49, 1162–1174. [PubMed: 30552024]

Briney B, Sok D, Jardine JG, Kulp DW, Skog P, Menis S, Jacak R, Kalyuzhniy O, de Val N, Sesterhenn F, et al. (2016). Tailored Immunogens Direct Affinity Maturation toward HIV Neutralizing Antibodies. Cell 166, 1459–1470. [PubMed: 27610570]

Casali P, and Notkins AL (1989). Probing the human B-cell repertoire with EBV: polyreactive antibodies and CD5+ B lymphocytes. Annual review of immunology 7, 513–535.

Cho A, and Wrammert J (2016). Implications of broadly neutralizing antibodies in the development of a universal influenza vaccine. Current opinion in virology 17, 110–115. [PubMed: 27031684]

Cohn M, and Langman RE (1990). The protecton: the unit of humoral immunity selected by evolution. Immunological reviews 115, 11–147. [PubMed: 2202659]

Crooks GE, Hon G, Chandonia JM, and Brenner SE (2004). WebLogo: a sequence logo generator. Genome research 14, 1188–1190. [PubMed: 15173120]

DeWitt WS, Lindau P, Snyder TM, Sherwood AM, Vignali M, Carlson CS, Greenberg PD, Duerkopp N, Emerson RO, and Robins HS (2016). A Public Database of Memory and Naive B-Cell Receptor Sequences. PloS one 11, e0160853. [PubMed: 27513338]

DiLillo DJ, Tan GS, Palese P, and Ravetch JV (2014). Broadly neutralizing hemagglutinin stalk-specific antibodies require FcgammaR interactions for protection against influenza virus in vivo. Nat Med 20, 143–151. [PubMed: 24412922]

DiLillo DJ, Palese P, Wilson PC, and Ravetch JV (2016). Broadly neutralizing anti-influenza antibodies require Fc receptor engagement for in vivo protection. The Journal of clinical investigation 126, 605–610. [PubMed: 26731473]

Dosenovic P, von Boehmer L, Escolano A, Jardine J, Freund NT, Gitlin AD, McGuire AT, Kulp DW, Oliveira T, Scharf L, et al. (2015). Immunization for HIV-1 Broadly Neutralizing Antibodies in Human Ig Knockin Mice. Cell 161, 1505–1515. [PubMed: 26091035]

Dosenovic P, Kara EE, Pettersson AK, McGuire AT, Gray M, Hartweger H, Thientosapol ES, Stamatatos L, and Nussenzweig MC (2018). Anti-HIV-1 B cell responses are dependent on B cell precursor frequency and antigen-binding affinity. Proceedings of the National Academy of Sciences of the United States of America 115, 4743–4748. [PubMed: 29666227]

Dosenovic P, Pettersson AK, Wall A, Thientosapol ES, Feng J, Weidle C, Bhullar K, Kara EE, Hartweger H, Pai JA, et al. (2019). Anti-idiotypic antibodies elicit anti-HIV-1-specific B cell responses. The Journal of experimental medicine. In press.

Duan H, Chen X, Boyington JC, Cheng C, Zhang Y, Jafari AJ, Stephens T, Tsybovsky Y, Kalyuzhniy O, Zhao P, et al. (2018). Glycan Masking Focuses Immune Responses to the HIV-1 CD4-Binding Site and Enhances Elicitation of VRC01-Class Precursor Antibodies. Immunity 49, 301–311. [PubMed: 30076101]

Erbelding EJ, Post D, Stemmy E, Roberts PC, Augustine AD, Ferguson S, Paules CI, Graham BS, and Fauci AS (2018). A Universal Influenza Vaccine: The Strategic Plan for the National Institute of Allergy and Infectious Diseases. The Journal of infectious diseases. 218, 347–354. [PubMed: 29506129]

Escolano A, Steichen JM, Dosenovic P, Kulp DW, Golijanin J, Sok D, Freund NT, Gitlin AD, Oliveira T, Araki T, et al. (2016). Sequential Immunization Elicits Broadly Neutralizing Anti-HIV-1 Antibodies in Ig Knockin Mice. Cell 166, 1445–1458. [PubMed: 27610569]

Fahnrich A, Krebbel M, Decker N, Leucker M, Lange FD, Kalies K, and Moller S (2017). ClonoCalc and ClonoPlot: immune repertoire analysis from raw files to publication figures with graphical user interface. BMC bioinformatics 18, 164. [PubMed: 28284194]

Fishwild DM, O'Donnell SL, Bengoechea T, Hudson DV, Harding F, Bernhard SL, Jones D, Kay RM, Higgins KM, Schramm SR, et al. (1996). High-avidity human IgG kappa monoclonal antibodies from a novel strain of minilocus transgenic mice. Nature biotechnology 14, 845–851.

Glaser L, Conenello G, Paulson J, and Palese P (2007). Effective replication of human influenza viruses in mice lacking a major alpha2,6 sialyltransferase. Virus research 126, 9–18. [PubMed: 17313986]

Guthmiller JJ, and Wilson PC (2018). Harnessing immune history to combat influenza viruses. Current opinion in immunology 53, 187–195. [PubMed: 29890370]

Hanley JA, and McNeil BJ (1983). A method of comparing the areas under receiver operating characteristic curves derived from the same cases. Radiology 148, 839–843. [PubMed: 6878708]

He W, Tan GS, Mullarkey CE, Lee AJ, Lam MM, Krammer F, Henry C, Wilson PC, Ashkar AA, Palese P, et al. (2016). Epitope specificity plays a critical role in regulating antibody-dependent cell-mediated cytotoxicity against influenza A virus. Proceedings of the National Academy of Sciences of the United States of America 113, 11931–11936. [PubMed: 27698132]

Henry Dunand CJ, and Wilson PC (2015). Restricted, canonical, stereotyped and convergent immunoglobulin responses. Philosophical transactions of the Royal Society of London Series B, Biological sciences 370.

Impagliazzo A, Milder F, Kuipers H, Wagner MV, Zhu X, Hoffman RM, van Meersbergen R, Huizingh J, Wanningen P, Verspuij J, et al. (2015). A stable trimeric influenza hemagglutinin stem as a broadly protective immunogen. Science 349, 1301–1306. [PubMed: 26303961]

Jardine JG, Ota T, Sok D, Pauthner M, Kulp DW, Kalyuzhniy O, Skog PD, Thinnes TC, Bhullar D, Briney B, et al. (2015). Priming a broadly neutralizing antibody response to HIV-1 using a germline-targeting immunogen. Science 349, 156–161. [PubMed: 26089355]

Joyce MG, Wheatley AK, Thomas PV, Chuang GY, Soto C, Bailer RT, Druz A, Georgiev IS, Gillespie RA, Kanekiyo M, et al. (2016). Vaccine-Induced Antibodies that Neutralize Group 1 and Group 2 Influenza A Viruses. Cell 166, 609–623. [PubMed: 27453470]

Kanekiyo M, Wei CJ, Yassine HM, McTamney PM, Boyington JC, Whittle JR, Rao SS, Kong WP, Wang L, and Nabel GJ (2013). Self-assembling influenza nanoparticle vaccines elicit broadly neutralizing H1N1 antibodies. Nature 499, 102–106. [PubMed: 23698367]

Kipps TJ, Robbins BA, and Carson DA (1990). Uniform high frequency expression of autoantibody-associated crossreactive idiotypes in the primary B cell follicles of human fetal spleen. The Journal of experimental medicine 171, 189–196. [PubMed: 1688607]

Kosik I, Angeletti D, Gibbs JS, Angel M, Takeda K, Kosikova M, Nair V, Hickman HD, Xie H, Brooke CB, et al. (2019). Neuraminidase inhibition contributes to influenza A virus neutralization by anti-hemagglutinin stem antibodies. The Journal of experimental medicine. 216, 304–316. [PubMed: 30683737]

Kong WP, Hood C, Yang ZY, Wei CJ, Xu L, Garcia-Sastre A, Tumpey TM, and Nabel GJ (2006). Protective immunity to lethal challenge of the 1918 pandemic influenza virus by vaccination. Proceedings of the National Academy of Sciences of the United States of America 103, 15987–15991. [PubMed: 17043214]

Krammer F, Garcia-Sastre A, and Palese P (2018). Is It Possible to Develop a "Universal" Influenza Virus Vaccine? Potential Target Antigens and Critical Aspects for a Universal Influenza Vaccine. Cold Spring Harb Perspect Biol 10, a028845. [PubMed: 28663209]

Lerner RA (2011). Rare antibodies from combinatorial libraries suggests an S.O.S. component of the human immunological repertoire. Molecular bioSystems 7, 1004–1012. [PubMed: 21298133]

Lingwood D, McTamney PM, Yassine HM, Whittle JR, Guo X, Boyington JC, Wei CJ, and Nabel GJ (2012). Structural and genetic basis for development of broadly neutralizing influenza antibodies. Nature 489, 566–570. [PubMed: 22932267]

Lonberg N (2005). Human antibodies from transgenic animals. Nature biotechnology 23, 1117–1125.

Lonberg N, Taylor LD, Harding FA, Trounstine M, Higgins KM, Schramm SR, Kuo CC, Mashayekh R, Wymore K, McCabe JG, et al. (1994). Antigen-specific human antibodies from mice comprising four distinct genetic modifications. Nature 368, 856–859. [PubMed: 8159246]

Lu Y, Welsh JP, and Swartz JR (2014). Production and stabilization of the trimeric influenza hemagglutinin stem domain for potentially broadly protective influenza vaccines. Proceedings of the National Academy of Sciences of the United States of America 111, 125–130. [PubMed: 24344259]

Mallajosyula VV, Citron M, Ferrara F, Lu X, Callahan C, Heidecker GJ, Sarma SP, Flynn JA, Temperton NJ, Liang X, et al. (2014). Influenza hemagglutinin stem-fragment immunogen elicits broadly neutralizing antibodies and confers heterologous protection. Proceedings of the National Academy of Sciences of the United States of America 111, E2514–2523. [PubMed: 24927560]

Masella AP, Bartram AK, Truszkowski JM, Brown DG, and Neufeld JD (2012). PANDAseq: paired-end assembler for illumina sequences. BMC bioinformatics 13, 31. [PubMed: 22333067]

McGuire AT, Gray MD, Dosenovic P, Gitlin AD, Freund NT, Petersen J, Correnti C, Johnsen W, Kegel R, Stuart AB, et al. (2016). Specifically modified Env immunogens activate B-cell precursors of broadly neutralizing HIV-1 antibodies in transgenic mice. Nature communications 7, 10618.

Nabel GJ, and Fauci AS (2010). Induction of unnatural immunity: prospects for a broadly protective universal influenza vaccine. Nature medicine 16, 1389–1391.

Nazarov VI, Pogorelyy MV, Komech EA, Zvyagin IV, Bolotin DA, Shugay M, Chudakov DM, Lebedev YB, and Mamedov IZ (2015). tcR: an R package for T cell receptor repertoire advanced data analysis. BMC bioinformatics 16, 175. [PubMed: 26017500]

Neumann G, Watanabe T, Ito H, Watanabe S, Goto H, Gao P, Hughes M, Perez DR, Donis R, Hoffmann E, et al. (1999). Generation of influenza A viruses entirely from cloned cDNAs. Proceedings of the National Academy of Sciences of the United States of America 96, 9345–9350. [PubMed: 10430945]

Pape KA, and Jenkins MK (2018). Do Memory B Cells Form Secondary Germinal Centers? It Depends. Cold Spring Harb Perspect Biol 10.

Pape KA, Maul RW, Dileepan T, Paustian AS, Gearhart PJ, and Jenkins MK (2018). Naive B Cells with High-Avidity Germline-Encoded Antigen Receptors Produce Persistent IgM(+) and Transient IgG(+) Memory B Cells. Immunity. 48, 1135–1143. [PubMed: 29884459]

Pappas L, Foglierini M, Piccoli L, Kallewaard NL, Turrini F, Silacci C, Fernandez-Rodriguez B, Agatic G, Giacchetto-Sasselli I, Pellicciotta G, et al. (2014). Rapid development of broadly influenza neutralizing antibodies through redundant mutations. Nature 516, 418–422. [PubMed: 25296253]

Paules C, and Subbarao K (2017). Influenza. Lancet 390, 697–708. [PubMed: 28302313]

Peterhoff D, and Wagner R (2017). Guiding the long way to broad HIV neutralization. Current opinion in HIV and AIDS 12, 257–264. [PubMed: 28257300]

Petrie JG, and Gordon A (2018). Epidemiological Studies to Support the Development of Next Generation Influenza Vaccines. Vaccines (Basel) 6.

Raymond DD, Bajic G, Ferdman J, Suphaphiphat P, Settembre EC, Moody MA, Schmidt AG, and Harrison SC (2018). Conserved epitope on influenza-virus hemagglutinin head defined by a vaccine-induced antibody. Proceedings of the National Academy of Sciences of the United States of America 115, 168–173. [PubMed: 29255041]

Rettig TA, Ward C, Bye BA, Pecaut MJ, and Chapes SK (2018). Characterization of the naive murine antibody repertoire using unamplified high-throughput sequencing. PloS one 13, e0190982. [PubMed: 29320559]

Scheid JF, Mouquet H, Feldhahn N, Seaman MS, Velinzon K, Pietzsch J, Ott RG, Anthony RM, Zebroski H, Hurley A, et al. (2009). Broad diversity of neutralizing antibodies isolated from memory B cells in HIV-infected individuals. Nature 458, 636–640. [PubMed: 19287373]

Schroeder HW Jr., and Cavacini L (2010). Structure and function of immunoglobulins. The Journal of allergy and clinical immunology 125, S41–52. [PubMed: 20176268]

Schroeder HW Jr., Hillson JL, and Perlmutter RM (1987). Early restriction of the human antibody repertoire. Science 238, 791–793. [PubMed: 3118465]

Shi B, Ma L, He X, Wang X, Wang P, Zhou L, and Yao X (2014). Comparative analysis of human and mouse immunoglobulin variable heavy regions from IMGT/LIGM-DB with IMGT/HighV-QUEST. Theor Biol Med Model 11, 30. [PubMed: 24992938]

Shlomchik MJ (2018). Do Memory B Cells Form Secondary Germinal Centers? Yes and No. Cold Spring Harb Perspect Biol 10.

Sok D, Briney B, Jardine JG, Kulp DW, Menis S, Pauthner M, Wood A, Lee EC, Le KM, Jones M, et al. (2016). Priming HIV-1 broadly neutralizing antibody precursors in human Ig loci transgenic mice. Science 353, 1557–1560. [PubMed: 27608668]

Sok D, Le KM, Vadnais M, Saye-Francisco KL, Jardine JG, Torres JL, Berndsen ZT, Kong L, Stanfield R, Ruiz J, et al. (2017). Rapid elicitation of broadly neutralizing antibodies to HIV by immunization in cows. Nature 548, 108–111. [PubMed: 28726771]

Steichen JM, Kulp DW, Tokatlian T, Escolano A, Dosenovic P, Stanfield RL, McCoy LE, Ozorowski G, Hu X, Kalyuzhniy O, et al. (2016). HIV Vaccine Design to Target Germline Precursors of Glycan-Dependent Broadly Neutralizing Antibodies. Immunity 45, 483–496. [PubMed: 27617678]

Sui J, Hwang WC, Perez S, Wei G, Aird D, Chen LM, Santelli E, Stec B, Cadwell G, Ali M, et al. (2009). Structural and functional bases for broad-spectrum neutralization of avian and human influenza A viruses. Nature structural & molecular biology 16, 265–273.

Tan HX, Jegaskanda S, Juno JA, Esterbauer R, Wong J, Kelly HG, Liu Y, Tilmanis D, Hurt AC, Yewdell JW, et al. (2019). Subdominance and poor intrinsic immunogenicity limit humoral immunity targeting influenza HA stem. The Journal of clinical investigation 129, 850–862. [PubMed: 30521496]

Tian M, Cheng C, Chen X, Duan H, Cheng HL, Dao M, Sheng Z, Kimble M, Wang L, Lin S, et al. (2016). Induction of HIV Neutralizing Antibody Lineages in Mice with Diverse Precursor Repertoires. Cell 166, 1471–1484. [PubMed: 27610571]

Tiller T, Busse CE, and Wardemann H (2009). Cloning and expression of murine Ig genes from single B cells. Journal of immunological methods 350, 183–193. [PubMed: 19716372]

Trombetta JJ, Gennert D, Lu D, Satija R, Shalek AK, and Regev A (2014). Preparation of Single-Cell RNA-Seq Libraries for Next Generation Sequencing. Current protocols in molecular biology / edited by Frederick M. Ausubel … [et al.] 107, 4 22 21–24 22 17.

Umotoy J, Bagaya BS, Joyce C, Schiffner T, Menis S, Saye-Francisco KL, Biddle T, Mohan S, Vollbrecht T, Kalyuzhniy O, et al. (2019). Rapid and Focused Maturation of a VRC01-Class HIV Broadly Neutralizing Antibody Lineage Involves Both Binding and Accommodation of the N276-Glycan. Immunity 51, 141–154 e146. [PubMed: 31315032]

Verkoczy L, Alt FW, and Tian M (2017). Human Ig knockin mice to study the development and regulation of HIV-1 broadly neutralizing antibodies. Immunological reviews 275, 89–107. [PubMed: 28133799]

Villar RF, Patel J, Weaver GC, Kanekiyo M, Wheatley AK, Yassine HM, Costello CE, Chandler KB, McTamney PM, Nabel GJ, et al. (2016). Reconstituted B cell receptor signaling reveals carbohydrate-dependent mode of activation. Scientific reports 6, 36298. [PubMed: 27796362]

Weaver GC, Villar RF, Kanekiyo M, Nabel GJ, Mascola JR, and Lingwood D (2016). In vitro reconstitution of B cell receptor-antigen interactions to evaluate potential vaccine candidates. Nature protocols 11, 193–213. [PubMed: 26741406]

Wheatley AK, Whittle JR, Lingwood D, Kanekiyo M, Yassine HM, Ma SS, Narpala SR, Prabhakaran MS, Matus-Nicodemos RA, Bailer RT, et al. (2015). H5N1 Vaccine-Elicited Memory B Cells Are Genetically Constrained by the IGHV Locus in the Recognition of a Neutralizing Epitope in the Hemagglutinin Stem. Journal of immunology 195, 602–610.

Whittle JR, Wheatley AK, Wu L, Lingwood D, Kanekiyo M, Ma SS, Narpala SR, Yassine HM, Frank GM, Yewdell JW, et al. (2014). Flow cytometry reveals that H5N1 vaccination elicits cross-reactive stem-directed antibodies from multiple Ig heavy-chain lineages. Journal of virology 88, 4047–4057. [PubMed: 24501410]

Wu NC, and Wilson IA (2017). A Perspective on the Structural and Functional Constraints for Immune Evasion: Insights from Influenza Virus. Journal of molecular biology 429, 2694–2709. [PubMed: 28648617]

Xu JL, and Davis MM (2000). Diversity in the CDR3 region of V(H) is sufficient for most antibody specificities. Immunity 13, 37–45. [PubMed: 10933393]

Yang ZY, Wei CJ, Kong WP, Wu L, Xu L, Smith DF, and Nabel GJ (2007). Immunization by avian H5 influenza hemagglutinin mutants with altered receptor binding specificity. Science 317, 825–828. [PubMed: 17690300]

Yassine HM, Boyington JC, McTamney PM, Wei CJ, Kanekiyo M, Kong WP, Gallagher JR, Wang L, Zhang Y, Joyce MG, et al. (2015). Hemagglutinin-stem nanoparticles generate heterosubtypic influenza protection. Nature medicine 21, 1065–1070.

Zhou T, Lynch RM, Chen L, Acharya P, Wu X, Doria-Rose NA, Joyce MG, Lingwood D, Soto C, Bailer RT, et al. (2015). Structural Repertoire of HIV-1-Neutralizing Antibodies Targeting the CD4 Supersite in 14 Donors. Cell 161, 1280–1292. [PubMed: 26004070]

Highlights

- Generated mice with user-defined human antibody VH-genes and humanized CDRH3 diversity
- IGHV1-69 use enables elicitation of IgG against a ‘universal’ site on influenza
- A single flu immunogen elicited gene-encoded broadly neutralizing antibodies
- The response was achieved when IGHV1-69 B cells were titrated to human frequency

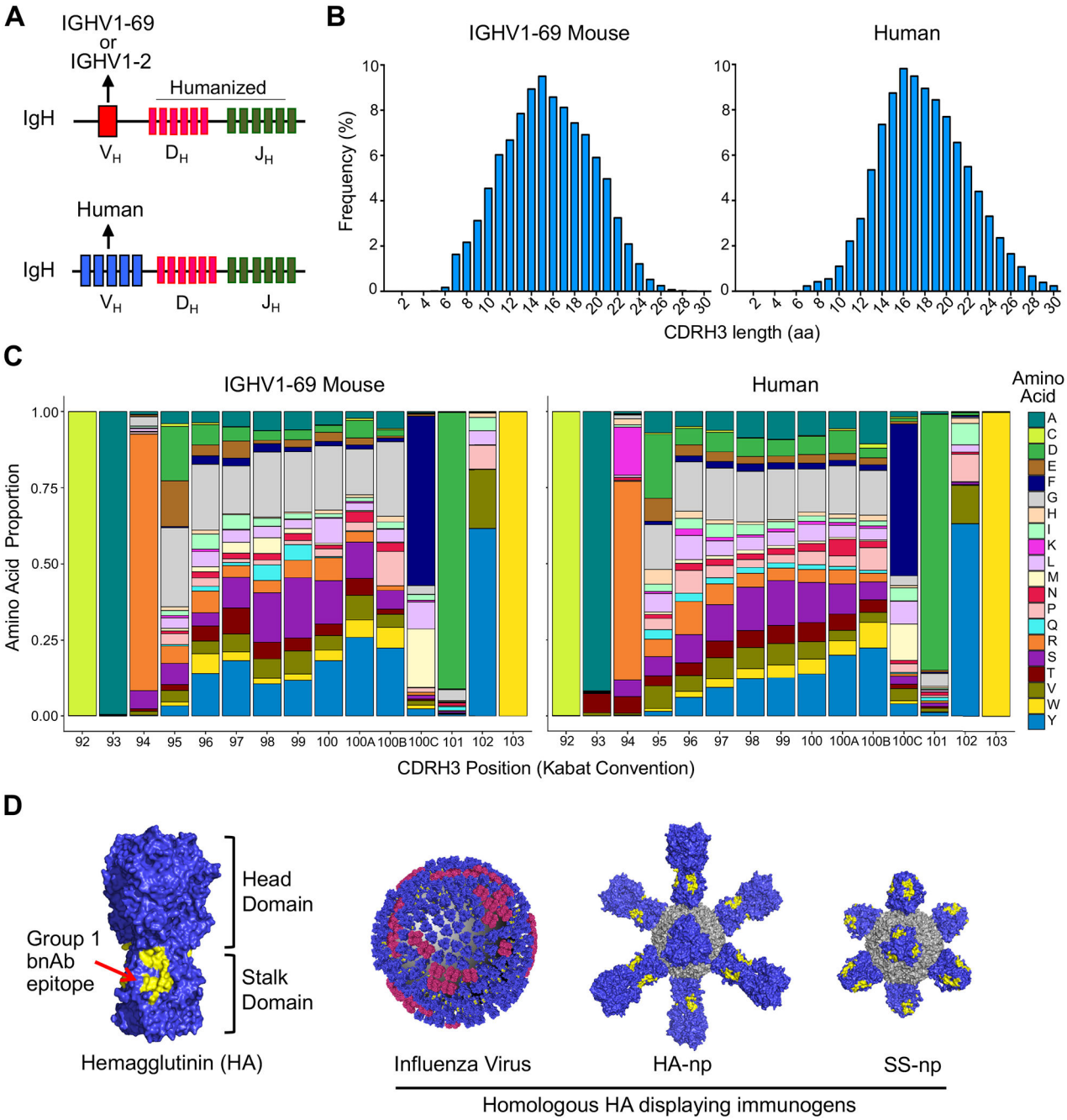

Figure 1. Generation of transgenic mice constrained to user-defined human V_H genes but with unconstrained humanized CDRH3 diversity.

(A) Illustration of the IgH locus in the V_H-gene restricted model as compared to humans.

(B) CDRH3 length distribution in the IGHV1-69 restricted mouse as compared to humans. BCR sequences obtained from naïve IgM B cells ($CD3^-/CD19^+/IgG^-/IgM^+$ cells; >5 million BCR reads from a single human patient and IGHV1-69 mouse). See Figure S2D for gating strategy. The human repertoire was publically available (DeWitt et al., 2016). See also Figure S2A–B for the IGHV1-2 genotype.

(C) CDRH3 amino acid composition from deep sequencing above in (B).

(D) Homologous HA immunogens used in this study: influenza virus (NC99); HA nanoparticle (HA-np); stalk-only nanoparticle (SS-np). The Group 1 bnAb epitope is marked in yellow. See also Figure S2

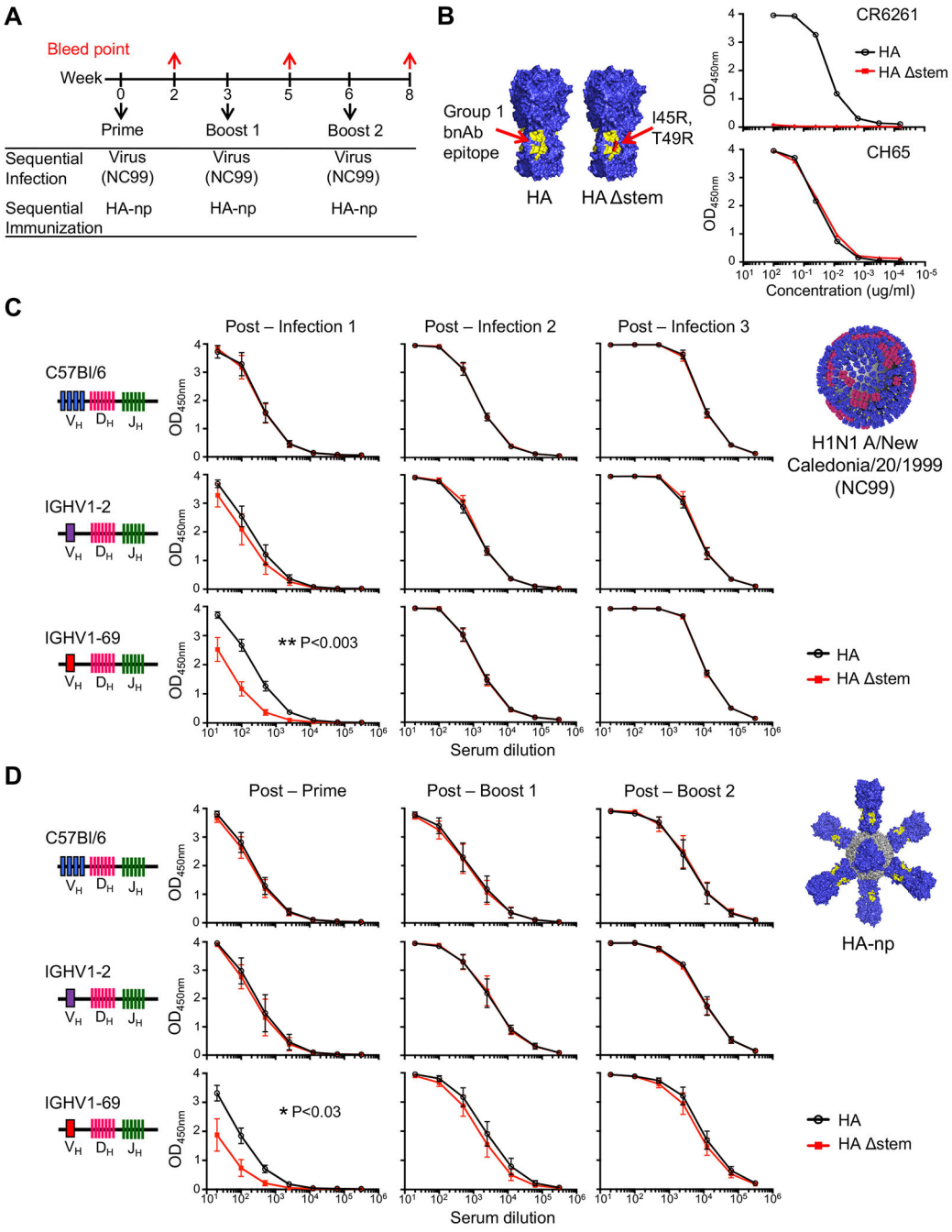

Figure 2. IGHV1-69 endows the antibody repertoire with a natural capacity to target the Group 1 bnAb epitope.

(A) Scheme for sequential immune challenge: NC99 virus infection or HA-np immunization.

(B) Group 1 bnAb epitope-targeting vs off-target IgG was assessed by reactivity to homologous HA (bnAb epitope: yellow) and HAΔstem probes (I45R, T49R point mutations: red). Binding curves for the prototypic IGHV1-69 bnAb CR6261 and the receptor binding site-specific bnAb CH65 are shown (performed in duplicate).

(C) Serum IgG response following sequential infection with NC99 in C57Bl/6, IGHV1-2 and IGHV1-69 genotypes. Targeting to the Group 1 bnAb epitope is denoted as reactivity to HA (black line) vs HAΔstem (red line). Mean and SEM are shown for each dilution curve (n = 5 mice/genotype).

(D) Serum IgG response following sequential immunization with HA-np. Mean and SEM are shown for each dilution curve (n = 5 mice/genotype).

For all responses area under the curve (AUC) was calculated using GraphPad PRISM software and these values were compared using the method of Hanley and McNeil (Hanley and McNeil, 1983) (*P<0.03, **P<0.003). Endpoint dilutions are presented in Figure S4A.

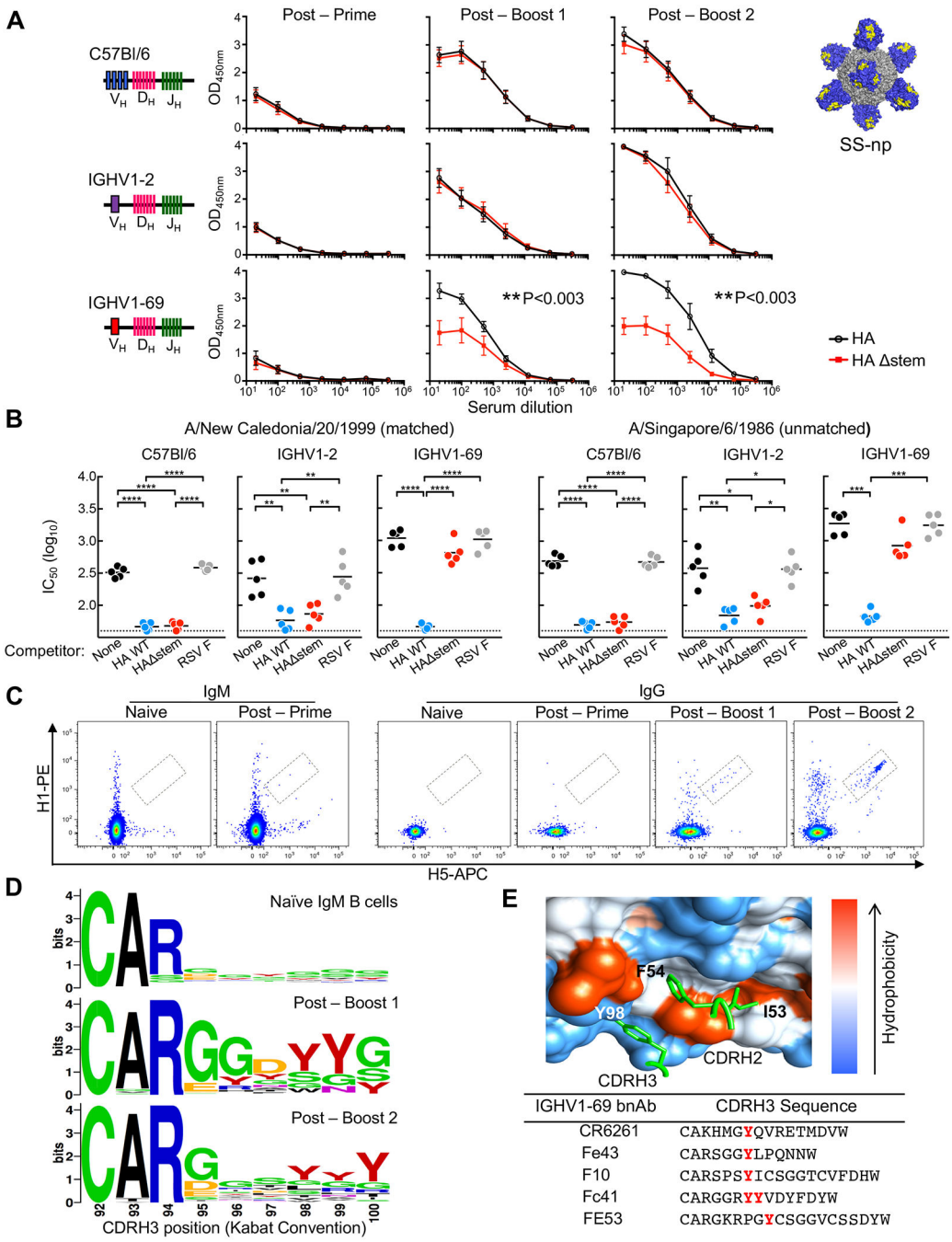

Figure 3. IGHV1-69-dependent amplification of the Group 1 bnAb epitope following sequential immunization with SS-np

(A) C57Bl/6, IGHV1-2 and IGHV1-69 animals were immunized three times with SS-np (weeks 0, 3, and 6) and serum IgG was measured for reactivity to HA vs HAΔstem probes two weeks after each injection (weeks 2, 5, and 8). Mean and SEM values are shown for each time point (n = 5 mice/genotype). AUC values were compared using the method of Hanley and McNeil (Hanley and McNeil, 1983) (**P<0.003, ***P<0.0003). Endpoint dilutions are presented in Figure S4A.

(B) In vitro neutralization activity of immune sera after SS-np immunization (n = 5 mice/genotype, post boost 2, bar = mean). The sera were pre-absorbed with competitors (HA, HAΔstem, or RSV F) and IC_{50} values were measured against A/New Caledonia/20/1999 (matched) and A/Singapore/6/1986 (unmatched) (*P<0.05, **P<0.01, ***P<0.001, ****P<0.0001, ANOVA with Tukey's Test) (see also Figure S4B).

(C) B cells targeting the Group 1 bnAb epitope were evaluated by flow cytometry both prior to and throughout the SS-np immunization regimen using cross-reactivity to H1-HA and H5-HA tetramers (Wheatley et al., 2015; Whittle et al., 2014). Dual-reactive IgM and IgG BCRs are marked by black boxes (see Figure S4C).

(D) CDRH3 sequences from dual reactive B cells isolated by FACS at post boost 1 (130 BCRs, n = 2 IGHV1-69 mice) and post boost 2 (140 BCRs, n = 2 IGHV1-69 mice), as compared to the naive IgM BCR repertoire (see also Figure 1).

(E) Tyr 98-100 is a hallmark of the human IGHV1-69 bnAb lineage, providing a key contact to the Group 1 IGHV1-69 bnAb epitope (PBD accession 3GBN) along with CDRH3 sequences from human IGHV1-69 bnAbs.

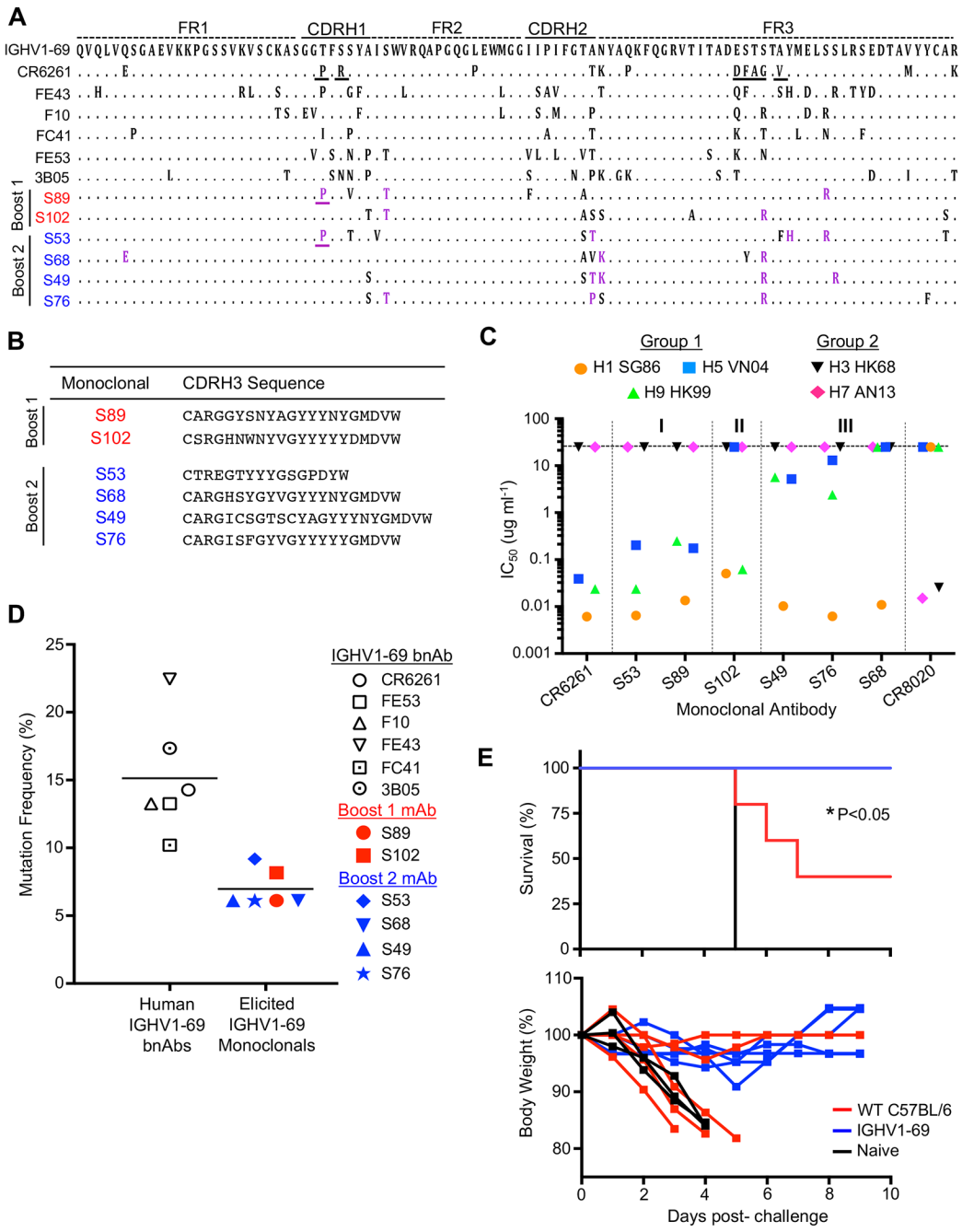

Figure 4. Vaccine-elicitation of bnAbs against Group 1 influenza viruses.

(A) SHM in six representative monoclonal antibodies (mAbs) isolated at post-boost 1 (red) and postboost 2 (blue) during the SS-np immunization regimen. Purple denotes mutations shared with known IGHV1-69 bnAbs and underlines denote changes known to confer neutralization breadth (Lingwood et al., 2012).

(B) CDRH3 sequences of the six representative mAbs.

(C) Neutralization of Group 1 (H1 SG86, H5 VN04, H9 HK99) and Group 2 (H3 HK68, H7 AN13) influenza pseudoviruses. IC50 values derived from n = 3 replicates were compared to

CR6261 (panGroup 1 neutralizer) and CR8020 (pan-Group 2 neutralizer). mAbs are grouped by ability to neutralize H1, H5, H9 (I); two of the three subtypes (II), or unmatched H1 only (III). In all cases a cut off of IC_{50} <1 ug/ml was applied (denoted by horizontal dotted line). See also Figure S4D–F.

(D) Percent SHM in the elicited mAbs as compared to human IGHV1-69 bnAbs. Line indicates mean.

(E) IGHV1-69 and control C57BL/6 (n = 5 mice/genotype) were immunized with SS-np and challenged with unmatched H5N1 virus. Weight loss and survival was evaluated (*P<0.05, Mantel-Cox test of survivorship between IGHV1-69 animals versus control C57Bl/6). The H5N1 dose given was lethal for naïve mice (black lines).

See also Figure S4 and S5.

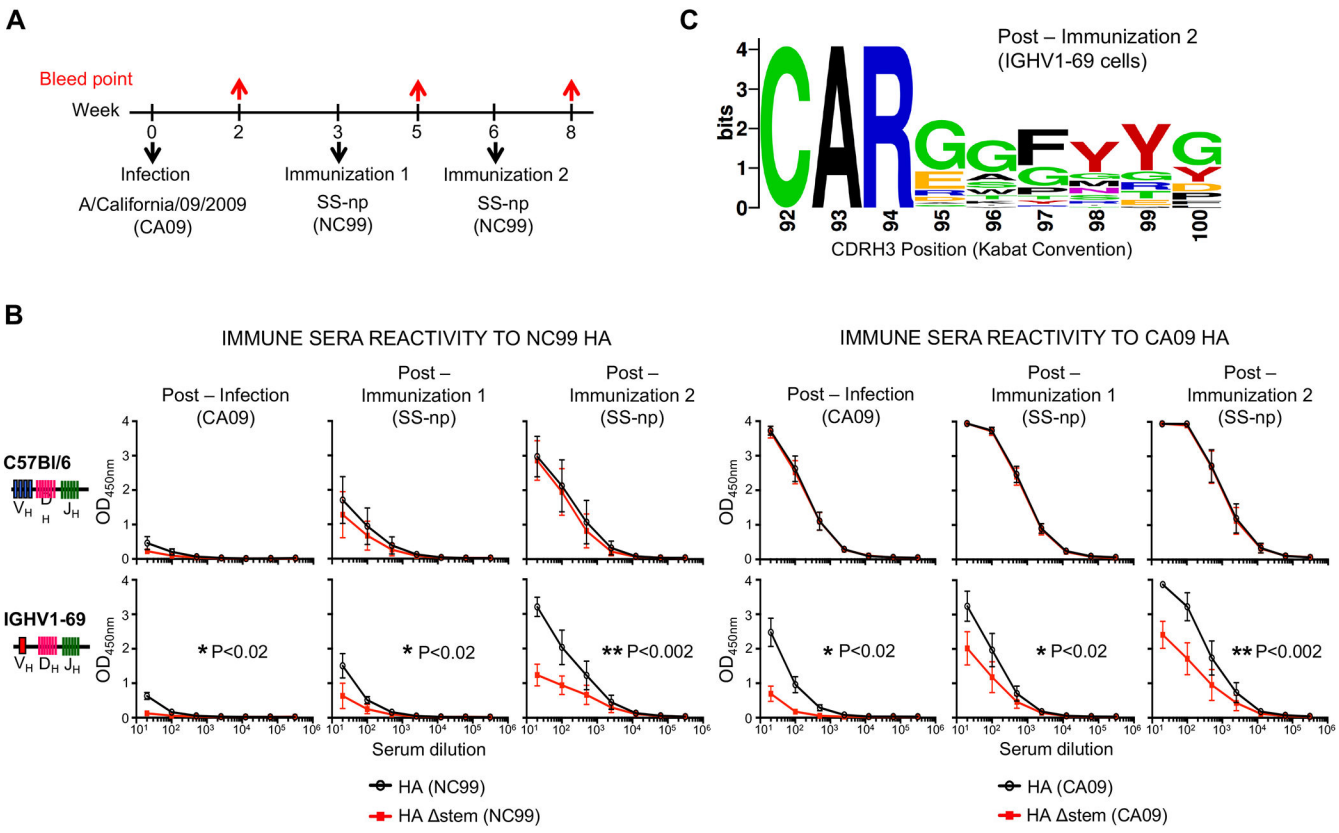

Figure 5. Pre-immunity to an H1N1 virus does not prevent IGHV1-69-dependent expansion of the bnAb response

(A) Infection and vaccination scheme: C57Bl/6 and IGHV1-69 mice were infected with a sublethal dose of H1N1 influenza virus (CA09) and then sequentially immunized with SS-np.

(B) Serum reactivity to HA vs HAΔstem probes matched either to CA09 or to SS-np (NC99) at week 2 (Post-Infection), 5 (Post-Immunization 1), and week 8 (Post-Immunization 2). Mean and SEM are presented for n = 4 mice/genotype. AUC values were compared using the method of Hanley and McNeil (Hanley and McNeil, 1983)(*P<0.02, **P<0.002).

C) CDRH3 amino acid sequences from 66 BCRs isolated from H1 and H5 dual-reactive B cells sampled at 2 weeks following Immunization 2 in one IGHV1-69 mouse.

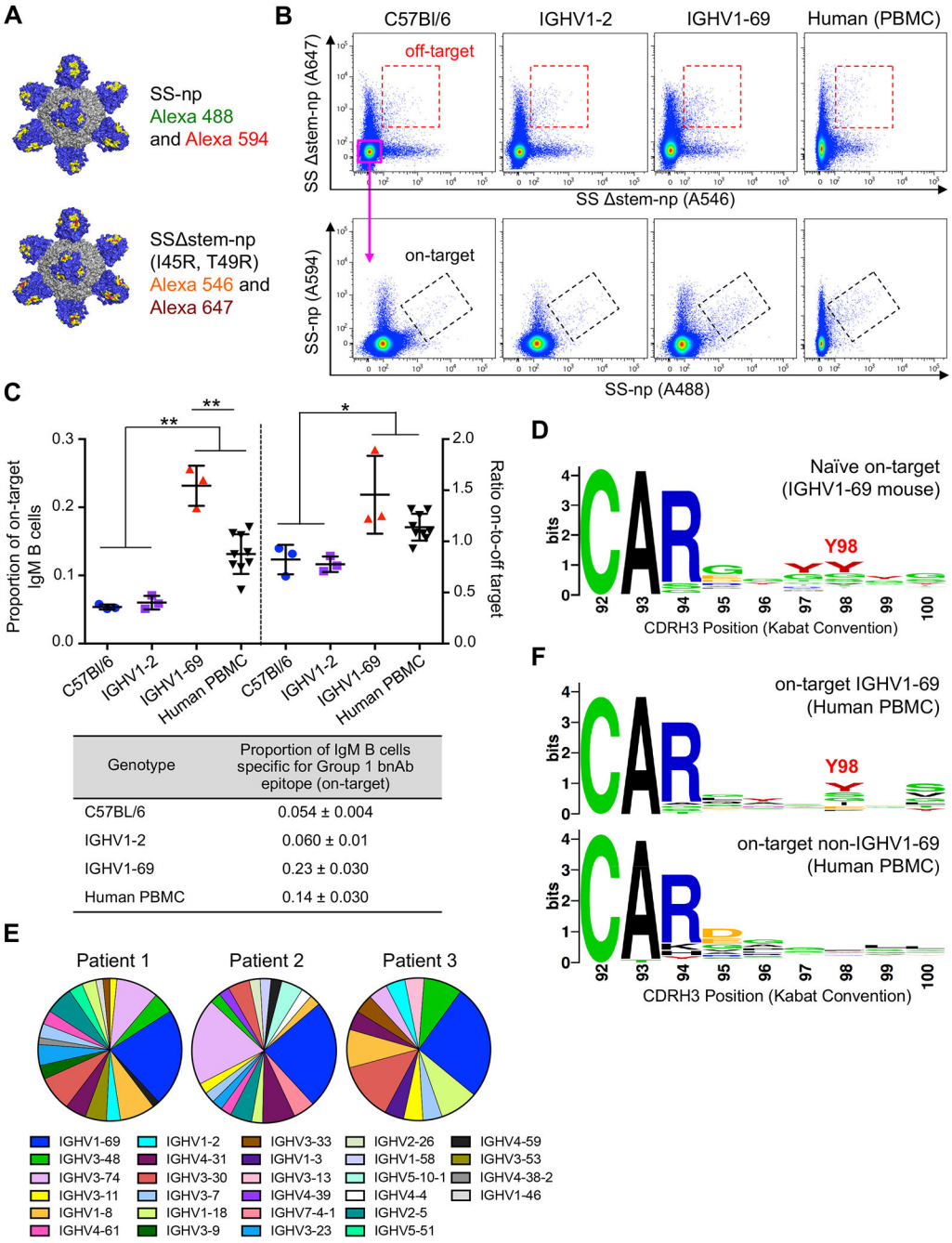

Genotype	Proportion of IgM B cells specific for Group 1 bnAb epitope (on-target)
C57BL/6	0.054 ± 0.004
IGHV1-2	0.060 ± 0.01
IGHV1-69	0.23 ± 0.030
Human PBMC	0.14 ± 0.030

Figure 6. V_H-endowed bnAb precursors in IGHV1-69 mice and humans

(A) Positive selector (SS-np Alexa 488 and SS-np Alexa 594) and negative selector (SS-np Δstem Alexa 546 and SS-np Δstem Alexa 647) B cell probes. Probe antigenicity and quality control is presented in Figures S6A–C.

(B) Representative SS-np probe reactivity to $CD3^-/CD19^+/IgG^-/IgM^+$ splenocytes (germline IgM B cells) from C57Bl/6, IGHV1-2 and IGHV1-69 mice, as well as human PBMC (see Figures 2SD and S6D for gating). Off-target IgM B cells bind both negative selector probes, but not positive selectors (specific for non-bnAb sites on SS-np); on-target

IgM B cells bind both positive selector probes but not negative selector probes (specific for the Group 1 bnAb epitope on SS-np).

(C) The proportion of on-target IgM B cells and the ratio of on-to-off target IgM B cells in the transgenic mice and in human PBMC. Data is presented as mean and SD for n = 3 mice/genotype and n = 9 human PBMC samples (*P<0.05, **P<0.03, ANOVA with Tukey's test). An accompanying table expressing the corresponding proportion of on-target B cells across all genotypes is also present.

(D) CDRH3 amino acid sequences isolated from on-target IgM B cells from IGHV1-69 animals (171 BCRs from one mouse).

(E) Percent V_H gene usage by on-target IgM B cells from human PBMC (Patients 1-3; 63, 41, and 23 BCRs, respectively).

(F) CDRH3 amino acid sequences from on-target IGHV1-69 B cells and non-IGHV1-69 B cells from human PBMC (Patients 1-3).

See also Figure S6.

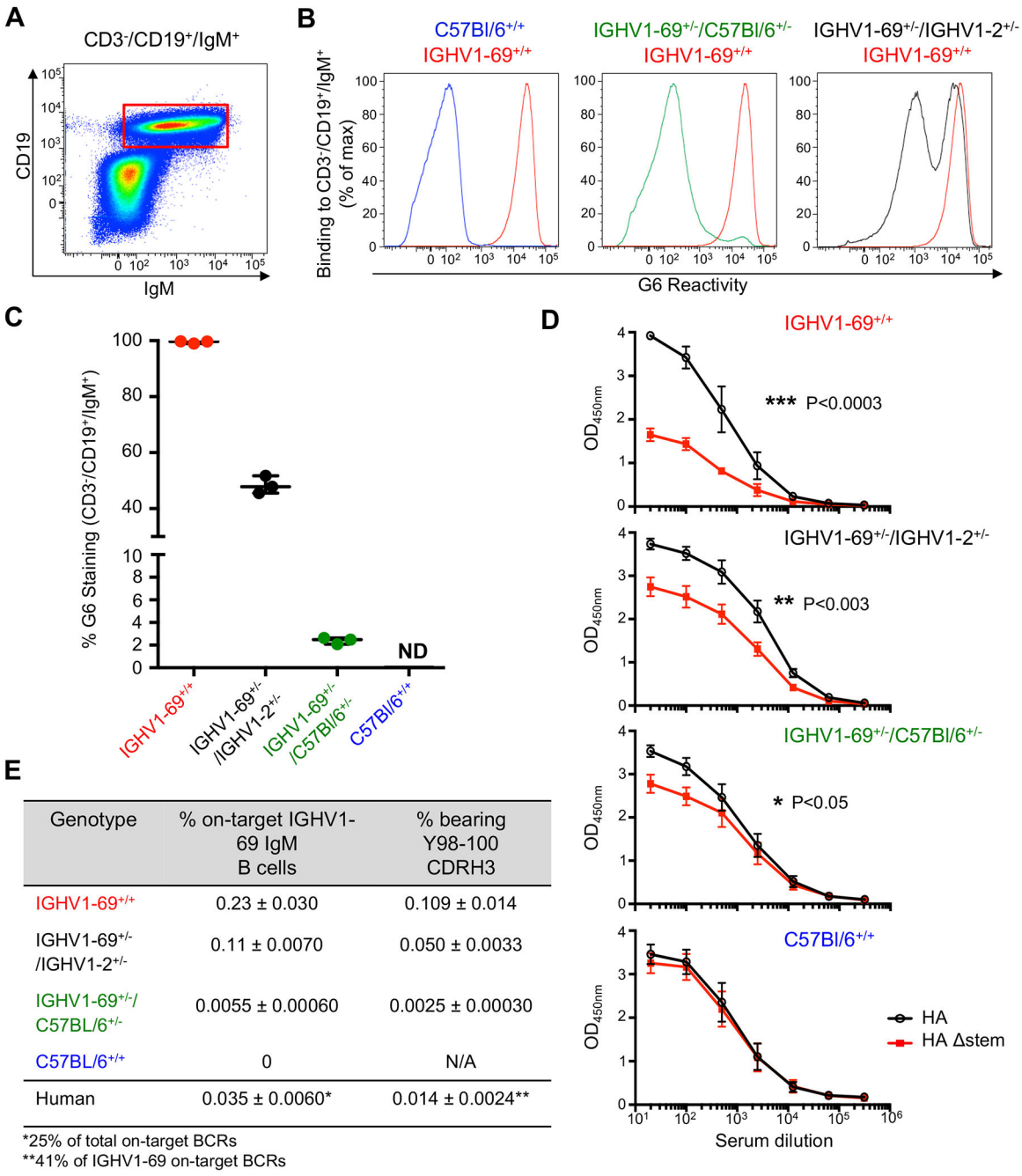

E

Genotype	% on-target IGHV1-69 IgM B cells	% bearing Y98-100 CDRH3
IGHV1-69$^{+/+}$	0.23 ± 0.030	0.109 ± 0.014
IGHV1-69$^{+/-}$ /IGHV1-2$^{+/-}$	0.11 ± 0.0070	0.050 ± 0.0033
IGHV1-69$^{+/-}$/ C57BL/6$^{+/-}$	0.0055 ± 0.00060	0.0025 ± 0.00030
C57BL/6$^{+/+}$	0	N/A
Human	0.035 ± 0.0060*	0.014 ± 0.0024**

*25% of total on-target BCRs
**41% of IGHV1-69 on-target BCRs

Figure 7. B cell dilution to human IGHV1-69 B cell frequency

(A) Gating strategy for naïve IgM B cells (CD3”/CD19^{+}/IgM^{+}) in the animal genotypes.

(B) IGHV1-69 usage, as measured by G6 reactivity to the BCR repertoires of C57Bl/6$^{+/+}$ (blue); IGHV1-69$^{+/-}$C57Bl/6$^{+/-}$ (green); IGHV1-69$^{+/-}$IGHV1-2$^{+/-}$ (black); and IGHV1-69$^{+/+}$ (red) genotypes.

(C) Proportion of G6 reactive IgM B cells in (B). Bar = mean and SD from n = 3 mice per genotype.

(D) Serum IgG reactivity to HA and HAΔstem probes in the genotypes following 3x sequential immunization with SS-np (Mean and SEM values presented for each dilution curve, n = 5 mice/genotype, Post-Boost 2). AUC values were compared using the method of Hanley and McNeil (Hanley and McNeil, 1983) (*P<0.05,**P<0.003, ***P<0.0003).
(E) The fraction of on-target IGHV1-69 IgM B cells in the animal genotypes versus the value measured in human PBMCs (see also Figure 6 and methods).
See also Figure S7